Trond Ivar Kopperud

Dynamic Current Rating of Power Transformers

The effect of maximum temperature and thermal ageing

June 2021

Master's thesis

Master's thesis

2021

Trond Ivar Kopperud

NTNU
Norwegian University of Science and Technology
Faculty of Information Technology and Electrical Engineering
Department of Electric Power Engineering

NTNU
Norwegian University of Science and Technology

NTNU
Norwegian University of Science and Technology

NTNU
Norwegian University of
Science and Technology

Dynamic Current Rating of Power Transformers

The effect of maximum temperature and thermal ageing

Trond Ivar Kopperud

Master of Science in Electric Power Engineering
Submission date: June 2021
Supervisor: Erling Ildstad

Norwegian University of Science and Technology
Department of Electric Power Engineering

This thesis is dedicated to my parents and brother.
For their endless support and encouragement.

Sammendrag

På grunn av forventet økning i kraftbehov og bruk av fornybare energikilder i fremtiden, er det et press for å undersøke metoder til å øke effektiviteten til eksisterende nettinfrastruktur. Smart grid konsepter slik som dynamisk termisk vurdering av belastningsevne representerer en mulighet for å utnytte den virkelige kapasiteten til transmisjonsnettet. Tradisjonelle statiske belastningsevner er basert på de verste værforholdene til kraftutstyr. Dynamiske vurderinger bruker målt belastning og miljøparametere for å bestemme den faktiske belastningsevnen i sanntid.

I denne oppgaven undersøkes dynamisk strømbelastning av krafttransformatorer. De kritiske parameterne for å bestemme den dynamiske vurderingen er viklingens hot-spot temperatur og papirisolasjonens slitasje. En simuleringsmetodikk er utviklet i Matlab Simulink for å utføre dynamiske termiske beregninger. Metoden simulerer forventet forbigående temperaturer og termisk aldring i transformatoren. En 300 MVA krafttransformator blir undersøkt i diverse casestudier med forskjellige overbelastningsstrømmer og værforhold.

Resultatene viser at den undersøkte transformatoren kan overbelastes kontinuerlig med opptil 110% økt strøm, avhengig av omgivelsestemperaturen. Transformatoren kan betjenes trygt under 140°C. Høyere temperaturer kan føre til dannelse av gassbobler i transformatoroljen. Overbelastning med 50% og mer økt strøm overstiger anbefalingene for strømbelastning av store krafttransformatorer etter dagens industrielle standarder. Ettersom dynamiske vurderingssystemer for transformatorer blir mer utbredt i fremtiden, foreslås det at gjeldende belastningsanbefalinger bør revideres.

Studier av termisk aldring antyder at overbelastning med 50% økt strøm ved 0°C omgivelsestemperatur og mer reduserer levetiden til transformatoren. Derfor må det innføres en tidsbegrensning hvis transformatorkapasiteten skal bevares. Optimalisering av papirisolasjonens levetid er den viktigste utfordringen i implementering av dynamiske transformatorvurderinger. Det er stort potensiale for å øke kapasitetsbruken av transformatorer i regioner med kaldt vær som Norge.

Abstract

Due to expected increase in power demand and use of renewable energy sources in the future, there is a pressure to investigate methods to increase the efficiency of existing grid infrastructure. Smart grid concepts such as dynamic thermal ratings represent an opportunity to utilize the true capacity of the transmission network. Traditional static ratings are based on the worst weather conditions of power equipment. Dynamic ratings use measured load and environmental parameters to determine the actual loading capability in real-time.

In this thesis, dynamic current rating of power transformers is investigated. The critical parameters to assess the dynamic rating is the winding hot-spot temperature, and the paper insulation loss-of-life. A simulation methodology is developed in Matlab Simulink to conduct dynamic thermal rating calculations. The methodology simulates expected transient temperatures and thermal ageing in the transformer. A 300 MVA power transformer is examined in various case studies with different overload currents and ambient weather conditions.

Results show that the examined transformer can be overloaded continuously with up to 110% increased current, depending on the ambient temperature. The transformer can be operated safely under 140°C. Higher temperatures can lead to gas bubble formation in the transformer oil. Overloading with 50% and more increased current exceeds recommendations for current loading of large power transformers by present day industrial standards. As dynamic rating systems of transformers become more prevalent in the future, it is proposed that the current loading recommendations should be revised.

Thermal ageing studies suggest overloading with 50% increased current at 0°C ambient temperature and above reduces the life expectancy of the transformer. Therefore, a time limit must be introduced if the transformer capacity is to be preserved. Optimizing the paper insulation life is the main challenge in implementing dynamic transformer ratings. There is great potential for increasing capacity usage of transformers in cold weather regions like Norway.

Preface

This thesis concludes my M.S. degree in Electric Power Engineering at the Norwegian University of Science and Technology (NTNU), carried out during the spring semester of 2021.

I would like to thank my supervisor, Professor Erling Ildstad for his guidance during this thesis work period. A special thanks goes to my brother Bjørn Tore Kopperud for his support and proofreading my thesis. Lastly, I would like to extend my gratitude to the professors at NTNU for all the knowledge I have gained during my time at NTNU.

Trondheim, June 2021

Trond Ivar Kopperud

Table of Contents

List of Tables

List of Figures

List of Symbols

Symbol	Description	Unit
E_A	Activation energy	[kJ/mol]
E_r	Reference activation energy	[kJ/mol]
A	Environmental factor	[h$^-$1]
A_r	Reference environmental factor	[h$^-$1]
R	Universal gas constant	[J/(K· mol)]
F_{AA}	Ageing acceleration factor	
$F_{AA-m,a}$	Ageing acceleration factor when effects of moisture and air are included	
t	Time	[min]
i	Current	[A]
v	Voltage	[V]
R_{el}	Electrical resistance	[Ω]
C_{el}	Electrical capacitance	[F]
q	Heat transfer rate	[W]
θ	Temperature	[°C]
R_{th}	Thermal resistance	[°C/W]
C_{th}	Thermal capacitance	[J/°C]
C_{th-oil}	Thermal capacity of oil	[J/°C]
$R_{th,R}$	Nominal thermal resistance	[°C/W]
$R_{th-hs-boil,R}$	Thermal resistance between winding insulation surface and bottom-oil at rated load	[°C/W]
$R_{th-boil-air,R}$	Thermal resistance between bottom-oil and air at rated load	[°C/W]
n	Air exponent	
m	Oil exponent	
K	Load factor	[p.u.]
R	Ratio between load-losses and no-load losses at rated voltage	
τ_{toil}	Top-oil time constant	[min]
τ_{wdn}	Winding time constant	[min]
θ_{hs}	Hot-spot temperature	[°C]
θ_{boil}	Bottom oil temperature	[°C]
θ_{amb}	Ambient temperature	[°C]
ε	Selected criteria for $\theta_{hs-\varepsilon}$	
$\Delta\theta_{boil}$	Bottom oil rise temperature gradient	[K]
$\Delta\theta_{hs-boil}$	Hot-spot rise above bottom-oil temperature gradient	[K]
$\Delta\theta_{avg}$	Average oil rise temperature gradient	[K]
q_{fe}	No-load losses	[W]
q_{cu}	Load-losses	[W]
p	Constant used in Agboza model	
c_{wdn}	Heat capacity of winding material	[Ws/kgK]
m_{wdn}	Mass of coil assembly	[kg]
c_{fe}	Heat capacity of core	[Ws/kgK]
m_{fe}	Mass of tank and fittings	[kg]
m_t	Mass of tank and fittings	[kg]
k_{oil}	Correction factor for the oil in ONAF, ONAN, OF and OD cooling modes	
m_{oil}	Mass of oil	[kg]
c_{wdn}	Heat capacity of winding material	[Ws/kgK]
P_{wdn}	Winding losses	[W]
P_e	Relative winding eddy losses	[p.u.]
s	Current density	[A/mm^2]

Abbrevations

SCADA	=	Supervisory Control and Data Acquisition
IEEE	=	Institute of Electrical and Electronics Engineers
IEC	=	International Electrotechnical Commission
DTR	=	Dynamic Transformer Rating
STR	=	Static Transformer Rating
DLR	=	Dynamic Line Rating
ONAN	=	Oil Natural Air Natural
ONAF	=	Oil Natural-Air Force
OFAF	=	Oil Forced Air Force
OFOD	=	Oil Force-Air Force
ODAF	=	Oil Directed Air Force
DP	=	Degree of polymerization
LOL	=	Loss-of-life

Chapter 1

Introduction

1.1 Motivation

The Master thesis is a continuation of the specialization project work ”Dynamic rating of transformers” [1]. Relevant background information described in the project work is reused and amended with new information in the thesis work.

Due to expected increase in power demand and use of renewable energy sources in the future, there is a pressure to investigate methods to increase the efficiency of existing electric grid infrastructure [2]. Smart grid concepts such as dynamic thermal ratings represent an opportunity to utilize the true capacity of the transmission network [3].

Traditional static ratings of power equipment are based on the worst case weather conditions, and are therefore conservative estimates of its loading capability. Dynamic thermal ratings or real-time ampacities assess the actual rating of the equipment. This is done with the assistance of measured loads and environmental parameters. The information is often accessible through the Supervisory Control and Data Acquisition (SCADA) system of network utilites. Dynamic rating systems enable transmission system operators to use the true loading capability of power equipment in real-time. This opens up avenues for increasing power transfer in the electric grid, without much investment to existing infrastructure [4].

Industry organizations such as the Institute of Electrical and Electronics Engineers (IEEE) and the International Electrotechnical Commission (IEC) suggest the use of dynamic thermal models. These are applicable for three main power components in the electric grid: power lines, cables and transformers [4]. Findings in [5] suggested that using dynamic thermal ratings could increase the average current rating of power transformers from 1.06 to 1.10 times compared to the conservative static rating.

Power transformers account for the the largest share of capital investments in transmission substations. One of the advantages of applying thermal models to transformers is that the parameters are available from conventional heat run tests performed by the manufacturer. One of the key parameters tied to the life expectancy of the transformer is the winding hot-spot temperature [6].

The life expectancy of the transformer relates to the rate of deterioration of the insulation material [7]. The current load and the weather conditions govern the heat balance of the transformer. This affects the life expectancy and thereby the transformer capacity. The winding hot-spot temperature and the resulting paper insulation loss-of-life are therefore critical parameters for assessing dynamic thermal ratings of transformers [2].

1.2 Task description

The objective of this thesis is to investigate dynamic current rating of power transformers. The main tasks are as follows:

- A literature survey, forming the base for dynamic thermal rating calculations and determining the effect of thermal ageing.
- Develop a simulation methodology for estimating transient expected maxiumum temperature and ageing due to selected transformer loads.
- Present selected case studies and discuss results and validity of the approach.

1.3 Thesis structure

The thesis is structured as follows:

- Chapter 2 gives an overview of the transformer, the dynamic rating definition and examples of dynamic transformer rating technologies.
- Chapter 3 presents the theoretical basis for calculation methods used to estimate transient temperatures and paper insulation loss-of-life.
- Chapter 4 presents a simulation methodology using Matlab Simulink.
- Chapter 5 presents results and discussions of selected case studies, including validity of the methodology.
- Chapter 6 presents concluding remarks and suggestions for future work.

Chapter 2

Literature review

In this chapter, a literature review is presented to give an overview of the transformer, the dynamic rating definition and some examples of dynamic transformer rating technologies.

2.1 Transformer introduction

The transformer is a static device that transfers electric energy from one circuit to another and changes the voltage level. The transfer of energy is done by using electromagnetic induction without changing frequency. Historically, the transformer was a key component in enabling the use of alternating current (AC) systems for the transmission and distribution of electric energy in the electric grid.

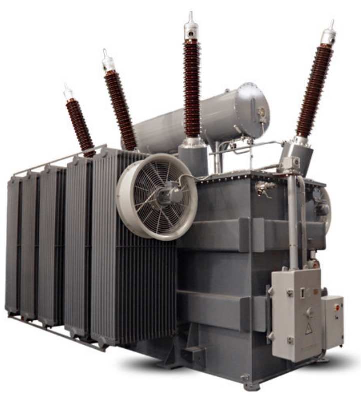

Figure 2.1: Oil-immersed power transformer [8]

The energy transfer process involves the electric energy first being received by the primary winding of the transformer equipment, where the electric energy is electromagnetically converted into magnetic energy, and subsequently reconverted back to electric energy in the secondary winding. The primary and secondary windings are not connected electrically due to this phenomena. Depending on the specific application, it is referred to as a step-down or step-up transformer. The step-down transformer downscales the secondary voltage relative to the primary voltage, while the step-up transformer upscales the secondary voltage relative to the primary voltage [9].

2.1.1 Heat generation and cooling modes

Heat is generated in the transformer as the equipment is loaded with current as a result of resistive and other losses. The losses are generated in the transformer windings. This heat is transferred away from the windings to the oil in the transformer, which is used as a cooling medium. Transformer oil does not degrade significantly at operating temperatures below 140°C. The paper insulation material in the transformer begins degrading at operating temperatures above 80°C. As the operating temperature exceeds 90°C and more, the degradation increases more severely [10]. Larger transformers use heat exchangers such as radiators that are mounted beside the oil tank to cool the oil. Table 2.1 below lists several cooling modes used by transformers.

Table 2.1: Cooling modes [11]

Cooling class	Definition
ONAN	Oil Natural-Air Natural
ONAF	Oil Natural-Air Force
OFAF	Oil Force-Air Force
OFOD	Oil Force-Oil Directed

ONAN dissipates heat from the oil to the atmosphere. The oil is circulated naturally through the windings and heat exchanger. The heat exchanger is cooled externally with natural air. ONAF continues to use natural circulation of oil, but the air flow is forced to the surface of the heat exchanger by using fans, thus increasing the heat transfer rate. OFAF increases the heat transfer further by forcing oil circulation with pumps, and fans continue to blow air on the surface of the heat exchanger to maximize heat dissipation. When the oil circulation is forced through the windings, it is considered as ”Directed Flow” and identified by the ODAF cooling mode. Conversely the oil flow is considered to be ”Non-Directed” when it is forced to flow freely in the oil tank [11].

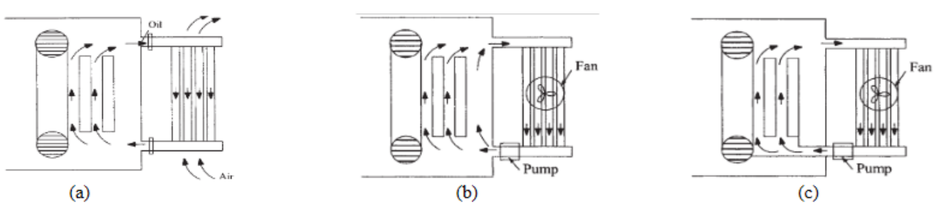

Figure 2.2: Cooling modes ONAN (a), OFAF (b) and ODAF (c) [12]

2.2 Dynamic transformer rating

Before the introducing the dynamic transformer rating (DTR), it may be insightful to review the definition of the static transformer rating (STR). The STR is a conservative rating based on the worst case operating conditions of the transformer equipment. This is known as the steady-state rating, as there is no specified time limit to the rating. Commonly it is also referred to as the name-plate rating of the equipment, given in volt-amperes (VA) or amperes (A). Figure 2.3 below shows the name-plate of a 800kVA transformer. The thermal rating is known as a transient or ”emergency” rating when there is a specified time limit (in minutes or hours) [13]. The IEEE C57.91 loading guide for oil-immersed transformers provides guidelines for operating the transformer at these emergency ratings. The loading guide also recommends that transformers with an average winding rise temperature 65°C is assigned a reference operating temperature 110°C. Thus, this operating temperature is the design value that is used when assigning the name-plate rating of the transformer. For the design the ambient temperature is assumed to be 30°C [7].

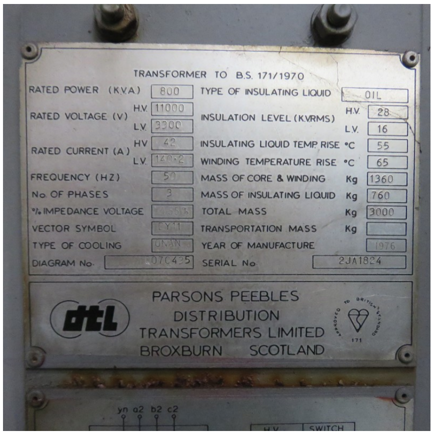

Figure 2.3: Name-plate of a 800kV distribution transformer [14]

The name-plate rating of the transformer with a 65°C average winding rise is defined as the loading the transformer is able to deliver continuously at:

- Rated frequency
- Rated secondary voltage
- Continuous winding hot-spot rise above ambient temperature 80°C
- Continuous ambient temperature 30°C

Adding the winding hot-spot rise and ambient temperature results in the 110°C operating temperature design value. This operating temperature is the hot-spot temperature of the transformer, and the limiting factor of the transformer loading capability [7].

With the conventional static rating properly defined, the dynamic rating can be introduced next. Lachman et al. defines the dynamic transformer rating as the following:

"The maximum loading which the transformer may acceptably sustain under time-varying load and/or environmental condition" [15].

The definition suggests that the true current rating of the transformer will be different from the conventional name-plate rating, as the real operating conditions differ from design conditions. Consider that on any given day where the ambient temperature is below the designated design value 30°C, the loading capability will be higher than the name-rating would imply. Conversely this also means that in the event that the ambient temperature exceeds 30°C, the loading capability will be lower than the name-plate rating. The usage of dynamic rating is dependent on the local weather conditions. Real-time data is necessary to compute the dynamic rating as environmental conditions can change at any given time interval [16].

2.2.1 Risks when loading beyond name-plate rating

It is important to review the risks associated with increasing the current loading of the transformer beyond its conventional name-plate rating. The increased loading results in a higher hot-spot temperature during operation, which subsequently accelerates the ageing of the paper insulation in the transformer. In general, subjecting the equipment to increased stresses could damage the transformer. Some of the consequences from loading beyond the name-plate rating include:

- Winding, insulation and oil temperatures increase and could exceed critical levels.
- Leakage flux density outside the core increases, resulting in increased eddy-currents heating metallic parts.
- Temperature changes cause change in moisture and gas content in the insulation and oil.
- Bushings, tap-changers, cable-end connections and current transformers can exceed design values due to increased stresses.

The IEC-60076-7 loading guide issues recommendations for overloading the transformer with respect to limits to current loading and hot-spot temperature values. These are divided into three loading types: normal cyclic loading, long-time and short-time emergency loadings. The recommended current loadings are listed in Table 2.2 on the next page. Industrial standards recommend that these current load limits should not be exceeded even if the temperature limits are not reached [17].

Table 2.3 on bottom of the next page lists the maximum hot-spot temperature limits provided by IEC. When the transformer is operated under the emergency loading types, there is risk of hazard. During a short-time emergency load, the conductor hot-spot could increase to a level where the dielectric strength of the transformer is temporarily reduced.

Table 2.2: Recommended current loading limits applicable to loading beyond name-plate rating by IEC [17]

Loading type	Small transformers	Medium power transformers	Large power transformers
Normal cyclic loading			
Current [p.u.]	1.5	1.5	1.3
Long-time emergency loading			
Current [p.u.]	1.8	1.5	1.3
Short-time emergency loading			
Current [p.u.]	2.0	1.8	1.5

The reason is that hot-spot temperatures exceeding 140°C in a transformer with moisture content equals to 2% of the winding insulation, increases the likelihood of gas bubble formation in the oil. This in turn causes the loss of dielectric strength. In such circumstances this is weighed against the risk of potentially losing power supply in the electric grid, should the loss of dielectric strength result in a failure. The short-time emergency loadings are rarely used due to the risks, and the transformer should be disconnected from the electric grid to prevent failure. 140°C hot-spot temperature in normal cyclic loading and long-time emergency loading is therefore the upper temperature limit that the transformer can acceptably sustain in the context of dynamic transformer ratings [17].

Table 2.3: Maximum temperature limits applicable to loading beyond name-plate rating by IEC [17]

Loading type	Small Transformers	Large and medium power transformers
Normal cyclic loading		
Winding hot-spot temperature and metallic parts in contact with cellulosic insulation material [°C]	120	120
Other metallic hot-spot temperature (in contact with oil, aramid, paper, glass fibre materials) [°C]	140	140
Inner core hot-spot temperature [°C]	130	130
Top-oil temperature, in tank [°C]	105	105
Long-time emergency loading		
Winding hot-spot temperature and metallic parts in contact with cellulosic insulation material [°C]	140	140
Other metallic hot-spot temperature (in contact with oil, aramid, paper, glass fibre materials) [°C]	160	160
Inner core hot-spot temperature [°C]	140	140
Top-oil temperature, in tank [°C]	115	115
Short-time emergency loading		
Winding hot-spot temperature and metallic parts in contact with cellulosic insulation material [°C]		160
Other metallic hot-spot temperature (in contact with oil, aramid, paper, glass fibre materials) [°C]		180
Inner core hot-spot temperature [°C]		160
Top-oil temperature, in tank [°C]		115

2.3 Examples of dynamic transformer rating technologies

Dynamic transformer rating (DTR) technology is relatively new with few applications in real power systems. Dynamic line ratings (DLR) are being implemented on a large scale in the industry, while more research and work in general is necessary for DTR. DTR functions similarly to DLR, but the transformer is more complicated than power lines [18].

In 2011, the utility company Unison Networks began installing a DTR system on its catalogue of power transformers in the distribution grid in New Zealand. The utility company developed an in-house DTR system that was implemented on 50 power transformers with a name-plate rating above 5 MVA. The system uses network sensors that measure the load current, top-oil temperature, ambient temperature and also provides the cooling mode and tap position of the transformers. Figure 2.4 below shows a flowchart of the algorithm. These are sampled through the Supervisory Control and Data Acquisition (SCADA) system, and calculation methods from industrial standards are subsequently used to estimate the hot-spot temperature and loss-of-life of paper insulation. The in-house algorithm then determines a real-time DTR based on these parameters. Thermal models from industrial standards use parameters that can be found by running conventional heat-run tests of the transformer. The Unison DTR system stores these parameters as they differ between the individual transformers in their portfolio [16].

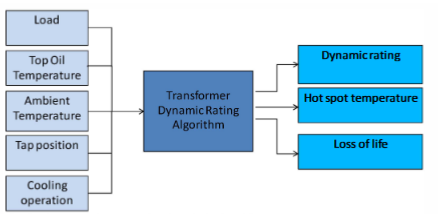

Figure 2.4: Flowchart for DTR algorithm used by Unison Networks [16]

Daminov et al. [19] investigated the DTR concept as a control task by employing receding horizon control (RHC) or model predictive control. In short, the RHC is a closed-loop system that that treats the thermal model from industrial standards as an object that is subjected to an optimization task. The control system is fed a forecasted daily load profile as an input and predicts the trajectory of the loading cycle, with limits to hot-spot temperature and paper insulation loss-of-life as the optimization constraints for the control system.

Zarei et al. [2] investigated using DTR for a sizing approach. In 2016, a transformer used in wind power applications was monitored for the duration of the year. Load and ambient temperatures were measured, and thermal models from industrial standards were used to estimate hot-spot temperatures and subsequently calculate the loss-of-life for the time period. The findings showed loss-of-life amounted to 22% of the monitored year of operation. This enabled suggestions for improvements such as decreasing transformer size, increasing wind farm size, and increasing upper operating temperature limits.

Chapter 3

Theoretical background

In this chapter, the theoretical background for calculation methods used in the thesis are presented. First, methods to estimate transient temperatures temperatures are presented, followed by methods to estimate loss-of-life in paper insulation as a result of thermal ageing.

3.1 Hot-spot temperature

As the name implies, the hot-spot temperature is the temperature of the hottest sections of the transformer, located at the transformer windings. The hot-spot temperature quantity is of critical importance to estimate the transformers dynamic loading capability [21].

Computational fluid dynamics (CFD) can be used to estimate the hot-spot temperature. The CFD model simulates the heat distribution and oil flow in the transformer windings. This is done by using numerical software to model the electromagnetic, fluid and thermal fields in the equipment [22]. A requirement for applying this method is that the constructed model will need to be tailored towards the specific transformer design. Thus, a CFD approach to estimating hot-spot temperatures cannot be used for the purpose of online monitoring of the transformer. Online monitoring systems are considered to be independent from the equipment. Lastly, CFD modeling requires large amounts of computational power and is time-consuming [23].

Monitoring approaches to obtaining thermal ratings are divided into direct and indirect methods. Direct monitoring involves using sensors placed in the winding to measure the hot-spot temperature directly [24]. Direct measurement is the most accurate monitoring method, provided that sensors are available. However, one issue that should be noted is that the hottest section of the transformer winding is not necessarily where the sensor is located. This could result in measurement errors. One way to alleviate this concern is to place several sensors in the area where the hot-spot section is expected to be during the manufacturing process [25].

Indirect monitoring involves using available environmental data and thermal models defined by industrial standards such as IEC, IEEE or CIGRE. The ambient temperature is the key environmental parameter of interest for transformers [24]. According to the industrial standard IEC 60076-7 for liquid-immersed oil transformers, the thermal models are based on the following assumptions [17]:

- The temperature of the oil inside the tank increases linearly from the bottom to the top of the tank, regardless of cooling mode.
- The difference between the average winding temperature rise and average oil temperature rise is assumed to be constant.
- The hot-spot temperature is higher than the temperature rise at the conductor temperature rise at the top of the winding.

Thermal models will be used to estimate the hot-spot temperature for the purpose of the dynamic thermal rating studies.

3.1.1 Dynamic thermal models

The conventional thermal model described by the IEC industrial standard is based on modeling the top-oil temperature in the transformer, and adding the expected hot-spot temperature rise to obtain the hot-spot temperature [17]. Rather than using the IEC method, the hot-spot temperature will be estimated by using a dynamic thermal modeling approached proposed by Agboza [26] in a previous master thesis work. The Agboza model differs from the conventional model in that it employs two thermal models: one for estimating the bottom-oil temperature, and one for estimating the hot-spot temperature. In the following subsections, the theoretical basis for these models will be presented, aswell as the parameters needed to use the model. The dynamic transformer rating studies are intended to upon Agboza's work, and so the naming conventions will refer to the subscripts in his work for the sake of consistency.

Thermal equivalent circuit

The principle of the thermal-electrical analogy forms the basis for the dynamic thermal models. Table 3.1 below describes the relationship between thermal and electrical quantities.

Table 3.1: Thermal-Electrical analogy [27]

	Thermal	**Electrical**
Through variable	Heat transfer rate q [W]	Current i i [A]
Across variable	Temperature θ [°C]	Voltage v [V]
Dissipation element	Thermal resistance R_{th} [°C/W]	Electrical resistance R_{el} [Ω]
Storage element	Thermal capacitance C_{th} [J/°C]	Electrical capacitance C_{el} [F]

Considering the fundamental electrical laws that define the electrical resistance and capacitance quantities, these may be converted into thermal laws, replacing the electrical quantities with thermal ones. This is seen in the equations on the next page:

$$v = R_{el} \cdot i \quad and \quad i = C_{el} \cdot \frac{dv}{dt} \tag{3.1}$$

$$\theta = R_{th} \cdot q \quad and \quad q = C_{th} \cdot \frac{d\theta}{dt} \tag{3.2}$$

The thermal resistance could be non-linear because of heat transfer law, which is described by the following relation:

$$\theta = R_{th,R} \cdot q^{n} \tag{3.3}$$

This new quantity $R_{th,R}$ is the nominal thermal resistance, provided that values for the quantities θ, q and n are known. The exponent n is used to quantify the behaviour of the moving fluid in the transformer. When the exponent is described using the symbol n, the moving fluid is air, while the symbol m is used for oil. As heat is transferred through the steel wall of a transformer, the heat transfer that occurs will be proportional to the temperature difference across the wall. This assumes however that the cooling medium flows at a constant rate, which is not necessarily the case depending on which cooling mode is being used. Therefore, the possible non-linear heat transfer is described by the following relation:

$$q = \frac{1}{R_{th,R}} \cdot \theta^{1/n} \quad with \quad 1/n > 1.0 \tag{3.4}$$

The value of the exponent n is selected based on the cooling mode the transformer is operating with. In cooling modes where no fans are used, it is suggested that n = 0.8. In cooling modes where fans are used, the convection rate will not be dependent on temperature. Thus, the exponent n increases towards 1.0, resulting in a linear heat transfer [27].

3.1.2 Bottom-oil temperature estimation

In this subsection, the thermal model proposed by Agboza [26] to estimate the bottom-oil temperature is presented. The theory in the Agboza model is based on the works of Swift [27][28] with respect to bottom-oil temperature estimation. The bottom-oil temperature is described by a thermal circuit showcased in Figure 3.1 on the next page.

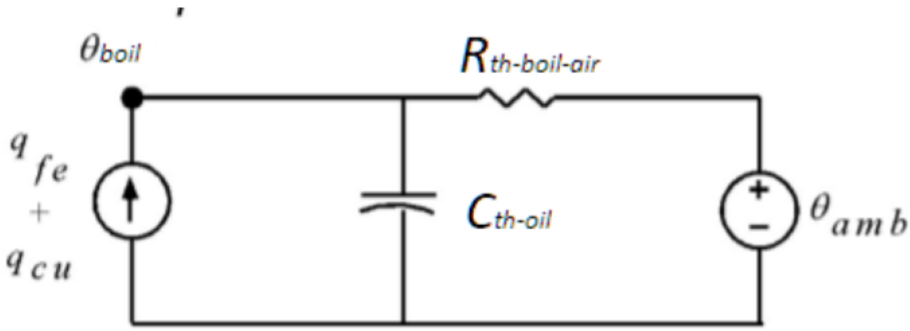

Figure 3.1: Thermal circuit for estimating bottom-oil temperature [26]

The thermal circuit may be described by the following differential equation:

$$q_{fe} + q_{cu} = C_{th-oil} \cdot \frac{d\theta_{boil}}{dt} + \frac{(\theta_{boil} - \theta_{amb})^{\frac{1}{n}}}{R_{th-boil-air,R}} \tag{3.5}$$

where:

- q_{fe} are the no-load losses [W]
- q_{cu} are the load-losses [W]
- C_{th-oil} is the thermal capacitance of the oil [J/°C]
- θ_{boil} is the bottom-oil temperature [°C]
- $R_{th-boil-air,R}$ is the non-linear thermal resistance between the bottom-oil and the air at rated load [°C/W]
- θ_{amb} is the ambient temperature [°C]
- n is an exponent that describes the non-linear heat transfer from oil to air.

In order to use the differential equation to estimate the bottom-oil temperature, some of the parameters are replaced. This is done so that rated data from the transformer can be used as inputs for the modeling intuitively. Replacing the parameters results in the following equation:

$$\frac{1 + K_{pu}^2 \cdot R}{1 + R} \cdot (\Delta\theta_{boil,R})^{\frac{1}{n}} = \tau_{boil} \cdot \frac{d\theta_{boil}}{dt} + (\theta_{boil} - \theta_{amb})^{\frac{1}{n}} \tag{3.6}$$

where:

- K_{pu} is the load factor [p.u.]
- R is the ratio between load-losses and no-load losses at rated load
- $\Delta\theta_{boil,R}$ is the bottom-oil rise above ambient temperature gradient at rated load

- τ_{boil} is the bottom-oil time constant [min]

Equation 3.6 serves as the theoretical basis for estimating the bottom-oil temperature which will be implemented in the next chapter. For more information on the mathematical procedure from Equation 3.5 to Equation 3.6, see Appendix A.

3.1.3 Hot-spot temperature estimation

In this subsection, the thermal model proposed by Agboza [26] to estimate the hot-spot temperature is presented. The theory in the Agboza model is based on the works of Pierce [29] with respect to hot-spot temperature estimation. The hot-spot temperature is described by a thermal circuit showcased in Figure 3.2 below.

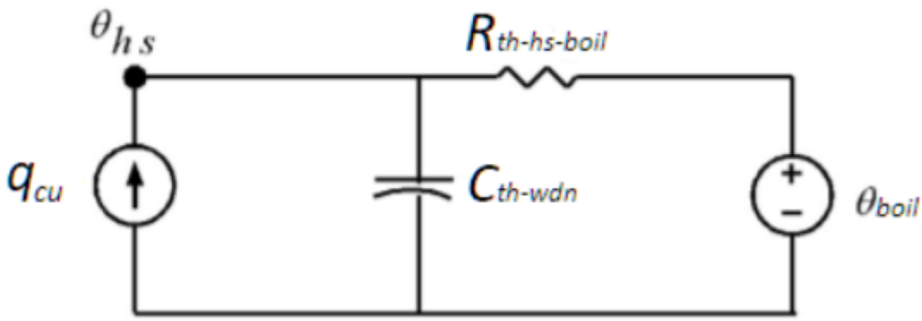

Figure 3.2: Hot-spot thermal circuit [26]

The thermal circuit may be described by the following differential equation:

$$q_{cu} = C_{th-wdn} \cdot \frac{d\theta_{hs}}{dt} + \frac{(\theta_{hs} - \theta_{boil})^{\frac{1}{m}}}{R_{th-hs-boil,R}} \tag{3.7}$$

where:

- q_{cu} is load losses [W]
- C_{th-wdn} is the thermal capacitance of the winding [J/°C]
- θ_{hs} is the hot-spot temperature [°C]
- $R_{th-hs-boil,R}$ is the thermal resistance between the surface of the winding insulation and the bottom-oil temperature at rated load [°C/W]
- θ_{boil} is the bottom-oil temperature [°C]
- m is an exponent which describes the non-linear heat transfer from winding to oil.

In order to use the differential equation to estimate the hot-spot temperature, some of the parameters are replaced. Similar to the bottom-oil modeling, this is done so that rated data from the specific transformer can be used as input data intuitively. Replacing the parameters results in the following equation:

$$K_{pu}^{\frac{2p}{m}} \cdot (\Delta\theta_{hs-boil,R})^{\frac{1}{m}} = \tau_{wdn} \cdot \frac{d\theta_{hs}}{dt} + (\theta_{hs} - \theta_{boil})^{\frac{1}{m}} \tag{3.8}$$

where:

- K_{pu} is the loading factor [pu.]
- $\Delta\theta_{hs-boil,R}$ is the hot-spot rise above bottom-oil temperature gradient at rated load [K]
- τ_{wdn} is the winding time constant [min]
- p is a constant. Note that p is given by IEEE loading guide [7].

Equation 3.8 serves as the theoretical basis for estimating the hot-spot temperature which will be implemented in the next chapter. For more information on the mathematical procedure from Equation 3.7 to Equation 3.8, see Appendix A.

3.1.4 Time constants

The oil and winding time constants used in the bottom-oil and hot-spot temperature models respectively can be calculated using equations described by the industrial standards. Note that as mentioned before, the conventional method from the standards estimate the top-oil temperature, and so according to IEC [17], the top-oil constant is expressed as the following:

$$\tau_{toil} = \frac{C_{th-oil,R} \cdot \Delta\theta_{toil,R}}{q_{tot,R} \cdot 60} \tag{3.9}$$

where:

- $\tau_{toil,R}$ is the top-oil time constant at rated load [min]
- $C_{th-oil,R}$ is the thermal capacitance of the oil at rated load [J/°C]
- $\Delta\theta_{toil,R}$ is the top-oil rise temperature gradient at rated load [K]
- $q_{tot,R}$ are the total amount of losses at rated load [W]

Susa explains that in order to obtain a time constant for the bottom-oil temperature, the top-oil temperature rise at rated load is substituted with the average temperature rise. Historically, it was assumed that the bottom-oil time constant was equal to that of the top-oil time constant. The reason being that older transformers designs had inlet pipes that went to the bottom of the tank, resulting in the bottom-oil mixing well as it flows to the windings. In newer transformer designs, the inlet pipes were instead placed around the middle section of the tank, resulting in a shorter bottom-oil time constant relative to the top-oil time constant [30]. Substituting the top-oil rise with the average rise results in the following expression, which can then be used in the Agboza model [26]:

$$\tau_{boil,R} = \frac{C_{th-oil,R} \cdot \Delta\theta_{avg,R}}{q_{tot,R} \cdot 60} \tag{3.10}$$

where:

- $\Delta\theta_{avg,R}$ is the average oil rise temperature gradient [K]

The thermal capacitance of the transformer oil is found by using the following expression according to IEC [17]:

$$C_{th-oil} = c_{wdn} \cdot m_{wdn} + c_{fe} \cdot m_{fe} + c_t \cdot m_t + k_{oil} \cdot m_{oil} \cdot c_{oil} \tag{3.11}$$

where:

- c_{wdn} is the heat capacity of the winding material (390 for Cu and 890 for Al) [Ws/kgK]
- m_{wdn} is the mass of the coil assembly [kg]
- c_{fe} is the heat capacity of the core = 468 [Ws/kgK]
- m_{fe} is the mass of the core [kg]
- c_t is the heat capacity of the tank and fittings = 468 [Ws/kgK]
- m_t is the mass of the tank and fittings [kg]
- k_{oil} is a correction factor for the oil in ONAF, ONAN, OF and OD cooling modes.
- m_{oil} is the mass of the oil [kg]

Next, the winding time constant may be calculated with the following equation according to IEC [17]:

$$\tau_{wdn} = \frac{m_{wdn} \cdot c_{wdn} \cdot \Delta\theta_{hs-boil,R}}{60 \cdot P_{wdn}} \tag{3.12}$$

where:

- m_{wdn} is the mass of the winding [kg]
- c_{wdn} is the heat capacity of the winding material (390 for Cu and 890 for Al) [Ws/kgK]
- $\Delta\theta_{hs-boil,R}$ is the hot-spot to bottom-oil temperature gradient at rated load [K]
- P_{wdn} are the winding losses at the specific load [W]

Alternatively, the winding time constant may also be calculated by using the following expressions for copper (Cu) and aluminium (Al) conductor materials respectively:

$$\tau_{wdn} = 2.75 \cdot \frac{\Delta\theta_{hs-boil,R}}{(1 + P_e) \cdot s^2} \;\; for \;\; Cu \tag{3.13}$$

$$\tau_{wdn} = 1.15 \cdot \frac{\Delta\theta_{hs-boil,R}}{(1 + P_e) \cdot s^2} \;\; for \;\; Al \tag{3.14}$$

where:

- $\Delta\theta_{hs-boil,R}$ is the hot-spot to bottom-oil temperature gradient at rated load [K]
- P_e is the relative winding eddy losses [p.u.]
- s is the current density at the specific load [A/mm^2]

3.2 Thermal ageing

In this section, the theoretical basis for assessing thermal ageing in the paper insulation of the transformer will be presented. First, an overview of the properties of paper insulation material and the degradation processes it is subjected to are presented. Next, calculation methods to estimate the paper insulation loss-of-life (LOL) are presented.

3.2.1 Paper insulation material properties

General kraft paper insulation used in transformers is composed of cellulose, hellicellulose and residual thiolignin that was not removed during the manufacturing process. Figure 3.3 showcases the chemical structure of the cellulose in the paper. The cellulose is comprised of polymeric chains of glucose units. The average number of these units per chain is known as the degree of polymerization (DP) [31].

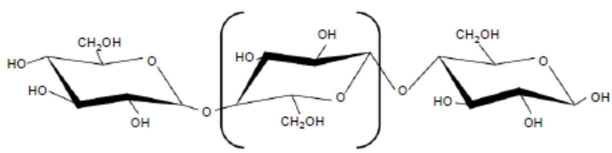

Figure 3.3: Cellulose chemical structure [17]

Most of the mechanical strength of the paper stems from fibrers and fibrils which is formed by these polymeric chains. The role of the hemicellulose and thiolignin is to connect these fibers together [31]. The DP-value is used as a measurement to evaluate the mechanical strength of the insulation material [17]. When the paper is subjected to elevated temperatures, the paper becomes brittle and loses its mechanical strength [11]. As the transformer is stressed during its operating lifetime, the cellulose in the paper deteriorates and reduces the DP-value as time goes on. Conventionally, new paper is said to have a DP-value of

1200. During the transformer manufacturing process, the paper is dried, which reduces the DP-value further down to 1000. When the DP-value reaches 200, the tensile strength of the paper is said to have been reduced to about 20% of its original value, where the transformer is considered to be at the end of its lifespan [31].

Degradation processes

The degradation that the paper is subjected is considered to come from three chemical reactions: hydrolysis, oxidation and pyrolysis. During operation, these three chemical reactions will occur simultaneously.

Hydrolysis is associated with the presence of moisture in the transformer. The process depends on carboxylic acids that are dissociated in water. As the cellulose material in the paper ages, both moisture content and carboxylic acids are formed, which in turn accelerates the hydrolysis process further. The drying of the transformer during manufacturing results in a moisture content of less than 0.5%. During the transformers lifespan, this moisture content can increase up to 5%.

Oxidation is associated with the presence of air in the insulation system. Depolarization from oxidation is initiated by hydroxyl-radicals (HO). These are produced by the decomposition of hydrogen peroxides (H_2O_2) or organic hydroperoxides $(ROOH)$. Hydrogen peroxides may for instance be formed by the presence of moisture or air in the insulation, which subsequently initiates the oxidation process.

Pyrolysis can occur without the presence of moisture, air or other contaminants that initiate the degradation of cellulose. Pyrolysis is considered to not be relevant at normal operating temperatures or overloading temperatures below 140°C [31].

Each of these degradation processes have an activation energy E and an environmental factor A associated to them. The activation energy governs to what extent the process is dependent on temperature [32]. Industrial standards aggregate these into one activation energy and environmental factor for hydrolysis and oxidation [17].

Thermally-upgraded paper

Most of the transformers operated by Statnett in Norway utilize so called thermally-upgraded paper [33]. The normal kraft paper, or non-thermally upgraded paper as its often referred to in industrial standards, undergoes a thermal upgrading process to improve its ageing performance. Investigations done by Sintef found that the nitrogen levels in the paper is considered to be an essential part of the upgrading process [32]. Example transformers that are studied in this work are assumed to be using thermally-upgraded paper. The theory presented in the following subsection encompasses calculation methods of thermal ageing with respect to the use of thermally-upgraded paper.

3.2.2 Thermal ageing estimation

The thermal ageing of the insulation material is modeled as a chemical reaction that adopts the Arrhenius reaction rate theory [7]. Both the IEC [17] and IEEE [7] industrial standards present calculation methods that neglect effects of moisture and air in the insulation system, leaving the hot-spot temperature as the only control variable. This is justified by the moisture and air contribution to the ageing being considered minimal due to newer oil preservation systems used in transformers.

In the IEEE loading guide, the ageing is initially presented as the 'per unit life', which is expressed by the following equation:

$$\text{Per Unit Life} = A \cdot e^{[\frac{B}{\theta_{hs}+273}]} \tag{3.15}$$

Where:

- A and B are constants
- θ_{hs} is the hot-spot temperature [°C]

The magnitudes of the constants are selected so that the reference operating temperature 110°C results in a per unit life equal to 1.0, resulting in the following equation:

$$\text{Per Unit Life} = 9.8 \times 10^{-18} \cdot e^{[\frac{15000}{\theta_{hs}+273}]} \tag{3.16}$$

Equation 3.16 serves as the foundation for expressions that describe the relative degradation of the insulating material dependent on the temperature profile of the transformer. IEC [17] refers to this as the relative ageing rate while IEEE calls it the the ageing acceleration factor. For the sake of consistency with IEEE the relative degradation is referred to as the ageing acceleration factor F_{AA}. When thermally-upgraded paper is used, the loading guide [7] lists the following equation:

$$F_{AA} = e^{[\frac{15000}{383} - \frac{15000}{\theta_{hs}+273}]} \tag{3.17}$$

As before with the 'per unit life' equation, a hot-spot temperature equal to 110°C results in the ageing acceleration factor being equal to 1.0. Therefore the ageing acceleration factor can be examined to observe the rate of ageing, depending on the present operating conditions. Note that Equation 3.17 does not include the effects of moisture and air. In the context of the dynamic rating studies in this work, it is of interest to include these effects. IEC [17] lists the following equation when moisture and air is taken into consideration:

$$F_{AA-m,a} = \frac{A}{A_r} \cdot e^{\frac{1}{R} \cdot (\frac{E_{A,r}}{\theta_{hs,r}+273} - \frac{E_A}{\theta_{hs}+273})} \tag{3.18}$$

Where:

- A is the selected environmental factor
- A_r is the reference environmental factor

- E_A is the selected activation energy.
- $E_{A,r}$ is the reference activation energy.
- R is the universal gas constant.
- θ_{hs} is the hot-spot temperature during operation.
- $\theta_{hs,r}$ is the reference hot-spot temperature (110°C for thermally-upgraded paper).

Table 3.2 below lists the numerical values of the activation energy and environmental factors. The reference values for the activation energy and environmental factors refer to the "free from air and 0.5% moisture" condition that the transformer is considered to be in after the manufacturing process. If the selected activation energy and environmental factor are also set to the reference values, then this neglects the effects of moisture and air, effectively resulting in the same calculation as Equation 3.17. When examining the effect of moisture and air, values from the other columns in the table can be selected.

Table 3.2: Activation energy (E_A) and environmental factor (A) for oxidation, hydrolysis by IEC [17]

Paper type/ ageing parameters		**Free from air and 0.5% moisture**	**Free from air and 1.5% moisture**	**Free from air and 3.5% moisture**	**With air and 0.5% moisture**
Thermally upgraded paper	A [h^{-}1]	1.6×10^4	3.0×10^4	6.1×10^4	3.2×10^4
	E_A [kJ/mol]	86	86	86	82

Lastly, the loss-of-life the insulating material is subjected to during operation can be calculated by integrating the ageing acceleration factor, yielding the following equation [17]:

$$LOL = \int_{t_1}^{t_2} F_{AA-m,a} \; dt \tag{3.19}$$

Where t_1 and t_2 represent the start and end of the time period respectively. The LOL parameter from Equation 3.19 will be implemented and calculated in the next chapters.

Chapter 4

Methodology

In this chapter, a simulation methodology using Matlab Simulink is presented. The methodology implements the calculation methods presented in Chapter 3. Those being methods for estimating transient bottom-oil and hot-spot temperatures, as well as the paper insulation loss-of-life from the resulting thermal ageing.

Before reviewing the methodology, some terminologies used in this chapter are presented for the sake of clarity to the reader. Figure 4.1 below showcases a signal builder block and a subsystem block in the simulink workspace. Subsystems are used to compress other blocks in the Simulink workspace to reduce clutter. These have a select amount of inputs and outputs depending on what is being compressed.

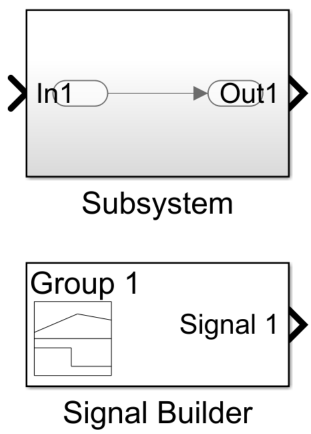

Figure 4.1: Simulink blocks

4.1 Overview of the simulation methodology

Figure 4.2 below outlines the steps involved in the simulation methodology.

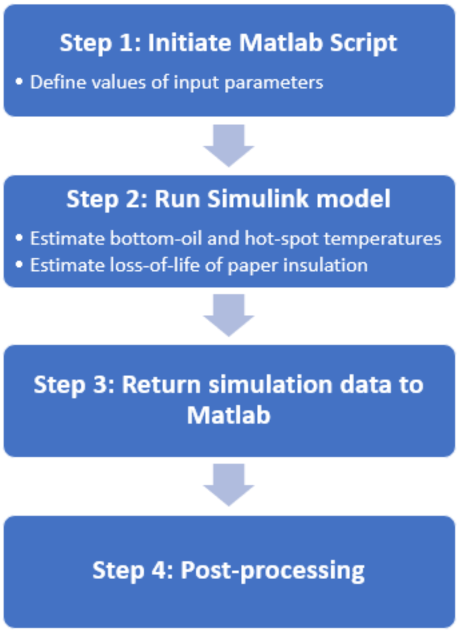

Figure 4.2: Simulation steps overview

The methodology can be divided into 4 steps. In the first step, a Matlab script is used to initiate the process. The script first defines fixed variables used in the Simulink model. These include transformer parameters used in thermal models, and activation energy and environmental factors used in thermal ageing modules. A constant ambient temperature is also defined as a fixed variable in the script. The second step begins with the script initiating the Simulink model by running a file named ”Simulink_DRT”. The Simulink model then performs the calculations to estimate transient temperatures and paper insulation loss-of-life. In the third step, the Simulink model returns data back to the Matlab workspace after the simulation has been completed. Lastly in the fourth step, the Matlab script performs post-processing of the simulation data. This includes creating graphical representations of the data, and exporting numerical values of interest for further analysis. For the source code of the Matlab script, see Appendix D. Figure 4.3 presents the complete Simulink model on the the next page.

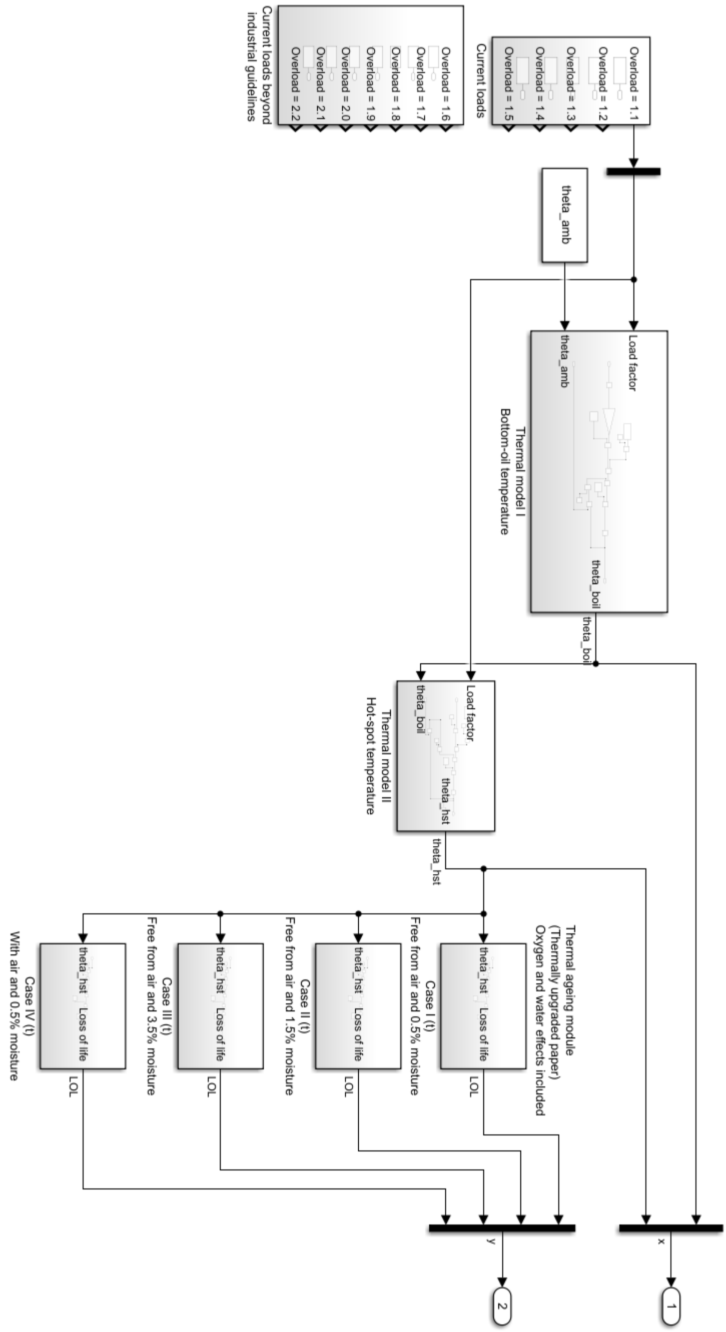

Figure 4.3: Simulink model

4.2 Simulink subsystems and theory implementation

In this section, the individual subsystems that the Simulink model is comprised of are examined more closely. Their functionality is explained step by step and how they relate to the theory presented in Chapter 3.

4.2.1 Current load selection

Before the Matlab script is run to initialize a simulation in step 1 in Figure 2.4, a current load is selected in the Simulink workspace. Two subsystems have been constructed for selecting current loads, as seen in Figure 4.4 below. This is done so that the Simulink model is easy to use and overloading conditions can be changed with minor intervention from the user. As current load values are presented in this chapter and onwards, note that the current loading is referred to by the per unit (pu.) system. The rated current load of a transformer equals that of 1.0 per unit (pu.) or 100% current. As an example, an initial load at 0.5 pu. equals the rated current multiplied with 0.5, while an overload at 1.5 pu. load equals the rated current multiplied with 1.5. The overload amounts to 50% increased current.

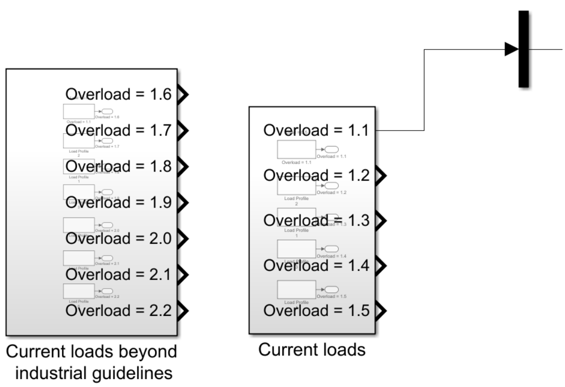

Figure 4.4: Subsystems for selection of current loads.

In specific example of Figure 4.4 above, the overload current is selected to be 1.1 pu. Inside the subsystems there are signal builder and output blocks, as seen in Figure 4.5 on the next page. The signal builders are used to describe the individual loading steps, and the output blocks serve as the connection point for selecting the current load. The right subsystem in Figure 4.4 contains loading steps with initial loads equal to 0.5 pu. and overloads ranging from 1.0-1.5 pu. These overloads adhere to recommendations from the industrial standards. The left subsystem in Figure 4.4 is used for selecting overloads ranging from 1.6-2.2 pu. These overloads exceed the industrial recommendations.

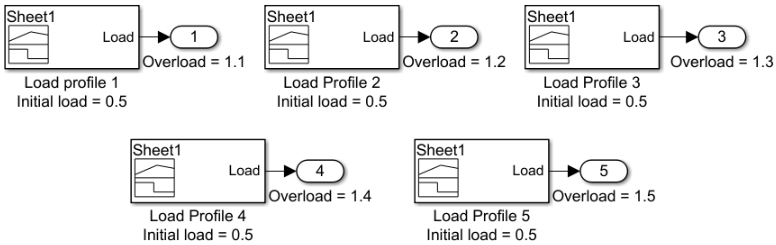

Figure 4.5: Signal builder and output blocks inside right subsystem in Figure 4.4. Initial loads equal 0.5 pu. and overloads range from 1.1-1.5 pu.

A loading step is shown in Figure 4.6 below, consisting of an initial load step at 0.5 pu. and an overload step at 1.1 pu. This is the load produced by the top left signal builder in Figure 4.5 above. The initial load is run for the first 100 time steps of the simulation. Note that time is shown by default in seconds in Simulink, but transformer parameters have been selected with respect to minutes. The first 100 minutes are used as a ramp-up time to to reach an approximate steady-state before the overloading condition is initiated. In other words, for the scope of this work, it is assumed that the hot-spot temperature is sufficiently steady-state prior to the overload being introduced at t = 100 minutes.

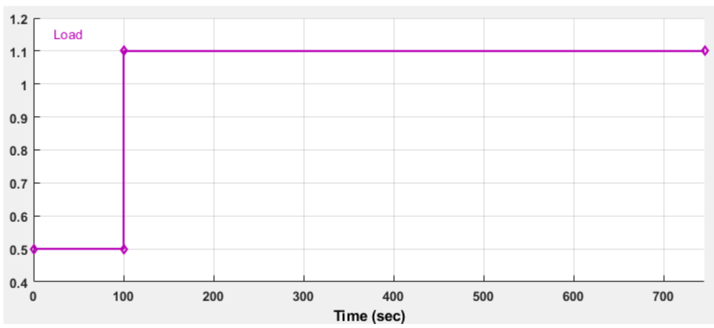

Figure 4.6: Load signal with initial load 0.5 pu. and overload 1.1 pu. Note that Simulink by default denotes time in seconds. The time steps are considered to be in minutes as the transformer parameters have been selected with respect to minutes for the simulation work.

4.2.2 Thermal model I - Bottom-oil temperature

As a simulation is intiated by running the Simulink model in step 2 in Figure 4.2, the first task of the model is to estimate bottom oil temperatures. Figure 4.7 on the next page showcases the subsystem representing the thermal model for estimating the bottom-oil temperature in the transformer. The subsystem has two inputs, one for the selected current load from Figure 4.4 and one for the ambient temperature. The ambient temperature is set as a constant value by the Matlab script. The output provides the estimated bottom-oil temperature.

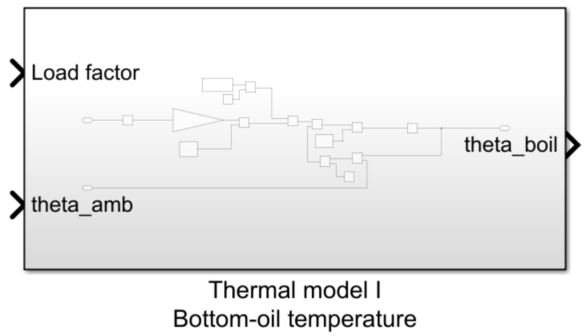

Figure 4.7: Subsystem for bottom-oil temperature estimation

In order to construct the thermal model inside the subsystem, the differential equation expressing the bottom-oil temperature in Equation 3.6 from Chapter 3 is re-written, so that the equation is a function of the derivative of the bottom-oil temperature. This results in the following equation, which serves as the theoretical basis for constructing the thermal model in Simulink.

$$\frac{d\theta_{boil}}{dt} = \frac{1}{\tau_{boil}}\left(\frac{1+K_{pu}^2}{1+R}(\Delta\theta_{boil,R})^{\frac{1}{n}} - (\theta_{boil} - \theta_{amb})^{\frac{1}{n}}\right) \tag{4.1}$$

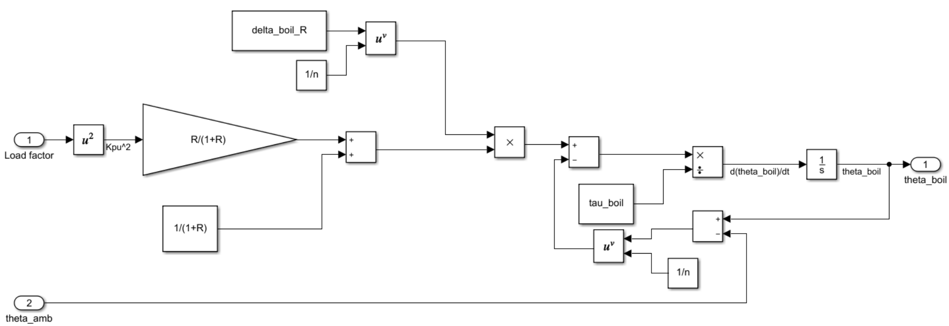

Figure 4.8: Bottom-oil calculation steps expressed inside subsystem in Figure 4.7

Figure 4.8 above showcases Equation 4.1 expressed in the Simulink workspace inside the subsystem. The bottom-oil temperature is obtained by integrating the derivative with an integrator block. An initial value for the temperature is necessary to initiate the computation.

4.2.3 Thermal model II - Hot-spot temperature

The second task in step 2 in Figure 4.2 is to estimate hot-spot temperatures. Figure 4.9 below showcases a subsystem which represents the thermal model used to estimate hot-spot temperatures. The subsystem has two inputs and two outputs. The inputs include the selected current load from Figure 4.4, and the bottom-oil temperature provided by the previous thermal model in Figure 4.7. The output is the estimated hot-spot temperature.

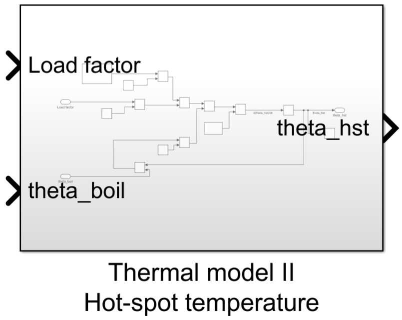

Figure 4.9: Subsystem for hot-spot temperature estimation

In order to construct the thermal model inside the subsystem, the differential equation expressing the hot-spot temperature in Equation 3.8 from Chapter 3 is re-written, so that the equation is a function of the derivative of the hot-spot temperature. This results in the following equation, which serves as the theoretical basis for constructing the thermal model in Simulink.

$$\frac{d\theta_{hs}}{dt} = \frac{1}{\tau_{wdn}}(K_{pu}^{\frac{2p}{m}}(\Delta\theta_{hs-boil,R})^{\frac{1}{m}} - (\theta_{hs} - \theta_{boil})^{\frac{1}{m}}) \tag{4.2}$$

Figure 4.10 below shows the inside of the subsystem, where Equation 4.2 is expressed in the Simulink workspace, and subsequently integrated to obtain the hot-spot temperature.

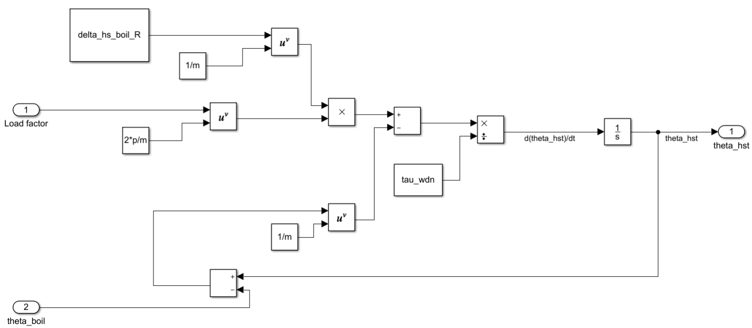

Figure 4.10: Hot-spot temperature calculation steps expressed inside subsystem in Figure 4.9

4.2.4 Thermal ageing modules

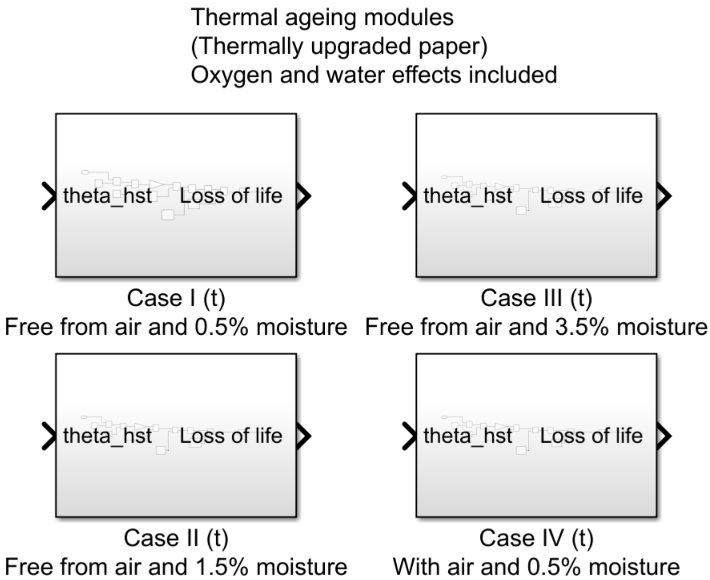

Figure 4.11: Subsystems for estimating loss-of-life when effects of air and moisture are included

The third task in step 3 in Figure 4.2 is to estimate the loss-of-life (LOL) of the paper insulation. Figure 4.11 above showcases subsystems for estimating the loss-of-life. The input is the hot-spot temperature provided by the thermal model in Figure 4.9. The output is the estimated loss-of-life in minutes. Four subsystems are included so that the loss-of-life is estimated for the four different moisture and air considerations in the columns of Table 3.2 in Chapter 3. Figure 4.12 below showcases the inside of one of the subsystems. The subsystem is constructed by referring to Equation 3.18 to calculate the ageing acceleration factor, and subsequently integrating it to obtain the LOL parameter from Equation 3.19.

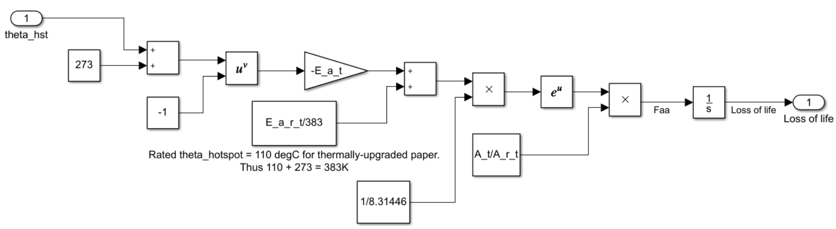

Figure 4.12: Loss-of-life calculation steps expressed inside one of the subsystems in Figure 4.11

4.2.5 Post-processing

In step 3 in Figure 4.2, the parameters of interest are collected and returned back to the Matlab workspace in the form of a signal. Figure 4.13 showcases these signal outputs, denominated signal x and signal y respectively. Signal x contains two data sets, the bottom-oil temperature and the hot-spot temperature respectively. Signal y contains four data sets, each representing loss-of-life data calculated by the thermal ageing modules with the respective air and moisture effects from Table 3.2 included.

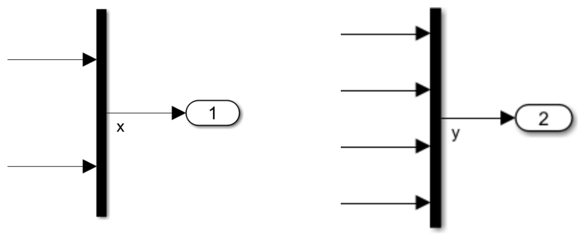

(a) Signal x output

(b) Signal y output

Figure 4.13: Signal outputs returning data to Matlab

Lastly in step 4 in Figure 4.2, the data sets are used for post-processing such as creating graphical representations and exporting numerical values of interest for further analysis.

Chapter 5

Results and discussion

In this chapter, numerical and graphical results from case studies performed with the developed Matlab Simulink methodology are presented and discussed. The chapter encompasses the following sections:

- An introduction study where a comparison is made between bottom-oil and hot-spot temperature results from the simulation methodology and results from previous thesis work by Agboza.
- Hot-spot temperature estimation during overloading conditions with various ambient temperatures. The hot-spot temperature is used to assess the dynamic thermal rating at the respective ambient temperatures.
- Thermal ageing assessment where loss-of-life is estimated during 24 hours of overloading with various ambient temperatures.
- Additional discussion remarks and validity of the simulation methodology.

5.1 Introduction study

An IEC example is studied and compared with the results found by the previous thesis work of Agboza [26]. This serves as a validation for the developed simulation methodology to estimate bottom-oil and hot-spot temperatures. The examined transformed is a 250 MVA power transformer using the Oil Natural-Air Force (ONAF) cooling mode. For more information about the transformer and the IEC example, see the relevant standard in [20]. For the numerical values of the transformer data parameters, see Appendix B.

Table 5.1: Comparison of results

Time [min]	Load [pu.]	Agboza results [26]		Simulink Model	
		θ_{boil} [°C]	θ_{hs} [°C]	θ_{boil} [°C]	θ_{hs} [°C]
0 - 190	1.0	39.5	85.6	39.8	85.9
190 - 365	0.6	33.4	61.2	33.5	61.3
365 - 500	1.5	52.9	121.8	52.8	121.7
500 - 705	0.3	31.3	45.4	31.4	45.5
705 - 730	2.1	44.2	138.9	44.6	138.9
730 - 745	0.0	40.9	46.2	42.1	55.8

Table 5.1 above lists the load steps, the results from the Agboza thesis, and the results from the Simulink model. Figure 5.1 below presents a graphical representation of the simulated temperatures. Comparing the results, the difference is little to none for the most part with the exception to the last row. This discrepancy could be explained by the sensitivity of the simulation. Consider that the load is reduced from 2.1 pu. down to 0.0 pu. The temperature drops dramatically each minute. Alternatively the result from the previous thesis work could be an error. Based on the comparison it is safe to say that the developed simulation methodology estimates the bottom-oil and hot-spot temperatures with sufficient accuracy.

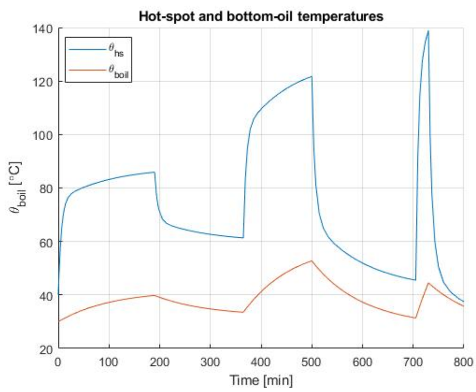

Figure 5.1: Hot-spot and bottom-oil temperatures

5.2 Dynamic thermal rating assessment

In this section, estimated hot-spot temperatures during overloading conditions with various ambient temperatures will be presented. These are used to assess the dynamic thermal rating of a power transformer at selected weather conditions. The example transformer that will be studied is a 300 MVA power transformer. Its nominal voltage ratings are $420 \pm 12\%$, 138 and 22 kV. The windings consist of a 420 kV primary winding, a 138 kV secondary winding, a regulating winding and a 22 kV tertiary winding. The oil flow in the winding is guided through the windings in a zig-zag pattern. The example transformer data used is obtained from the previous thesis work of Agboza [26]. For the numerical values of the transformer data parameters, see Appendix C. Parameters associated with the high voltage winding of the example transformer are selected for the studies. Table 5.2 summarizes the weather conditions in the examined case studies. Initial load before overload is selected to be 0.5 pu. As mentioned in Chapter 4, the first 100 minutes in the simulations are used as a ramp-up time for the initial load to reach an approximate steady-state prior to initiating overload. The transformer is overloaded for another 100 minutes to estimate sufficiently accurate steady-state values.

Table 5.2: Case studies

Case studies	**Ambient temperature [°C]**
Case 1: Extreme cold	-30
Case 2: Cold	-20
Case 3: Moderate cold	-10
Case 4: Chilling	0
Case 5: Moderate warm	10
Case 6: Warm	20
Case 7: Design conditions	30

5.2.1 Case 1: Extreme cold (-30°C)

In this first case study, the ambient temperature is set as -30°C. Figure 5.2 below showcases the hot-spot temperature results under overloading conditions ranging from 1.1-2.2 pu. Note that there are two red dashed lines in the graphical representation. The lower line denotes the reference operating temperature 110°C, and the upper line denotes the upper hot-spot temperature limit 140°C with respect to temperature guidelines from industrial standards mentioned in Chapter 2.

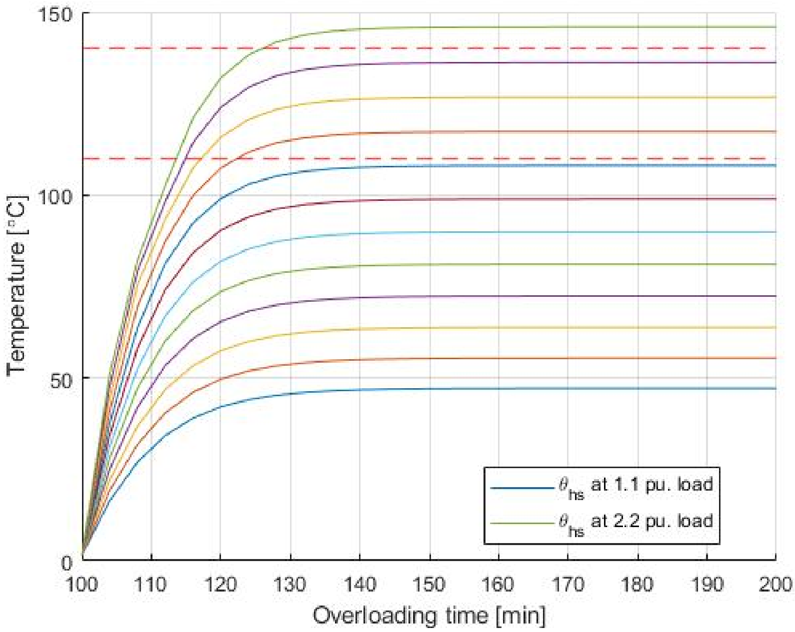

Figure 5.2: Hot-spot temperatures during overloading conditions. Overloads range from 1.1-2.2 pu. Lower red dashed line denotes 110°C and upper red dashed line denotes 140°C.

Looking at the lower dashed red line in Figure 5.2 above, the hot-spot temperature begins to exceed the reference temperature at 1.9 pu. load, which in turn results in thermal ageing occurring faster than nominal levels. Furthermore, the upper temperature threshold is exceeded at 2.2 pu. load, thus this load is not viable due to the risk of gas bubble formation in the transformer oil. 2.1 pu. is therefore the upper load limit that is safe to use continuously in these extreme cold weather conditions, with respect to temperature guidelines from industrial standards. However, this load step is several steps higher than the industrial guidelines for current loading mentioned in Chapter 2, which stated that the current loading of large power transformers should not exceed 1.5 pu. during short-time emergency loading.

5.2.2 Case 2: Cold (-20°C)

Increasing the ambient temperature to -20°C, results in higher hot-spot temperatures, and the strain on the transformer will be increased. Figure 5.3 below showcases the hot-spot temperature results under overloading conditions ranging from 1.1-2.1 pu. As before, the red dashed lines denote the reference operating temperature 110°C and the upper hot-spot temperature limit 140°C.

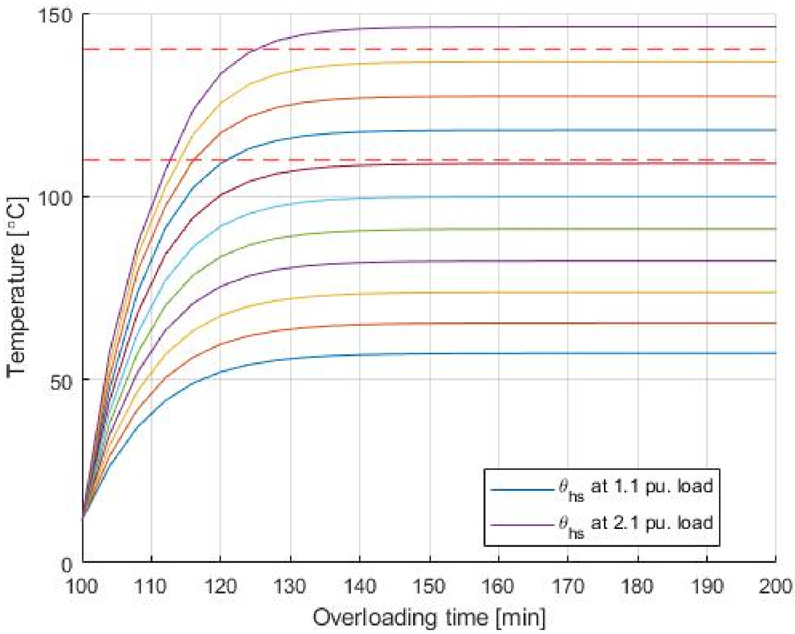

Figure 5.3: Hot-spot temperatures during overloading conditions. Overloads range from 1.1-2.1 pu. Lower red dashed line denotes 110°C and upper red dashed line denotes 140°C.

Looking at the lower red dashed line in Figure 5.3 above, the hot-spot temperature begins to exceed the reference temperature at 1.8 pu. load, which in turn results in thermal ageing occurring faster than nominal levels. Furthermore, the upper temperature threshold is exceeded at 2.1 pu. load, thus this load is not viable due to the risk of gas bubble formation in the transformer oil. 2.0 pu. is therefore the upper load limit that is safe to use continuously in these cold weather conditions, with respect to temperature guidelines from industrial standards. However, this load step remains several steps higher than the recommended 1.5 pu. load from the industrial standards with respect to current loading.

5.2.3 Case 3: Moderate cold (-10°C)

Increasing the ambient temperature to -10°C results in higher hot-spot temperatures, and puts further strain on the transformer. Figure 5.4 below showcases the hot-spot temperature results under overloading conditions ranging from 1.1-2.0 pu. As before, the red dashed lines denote the reference operating temperature 110°C and the upper hot-spot temperature limit 140°C.

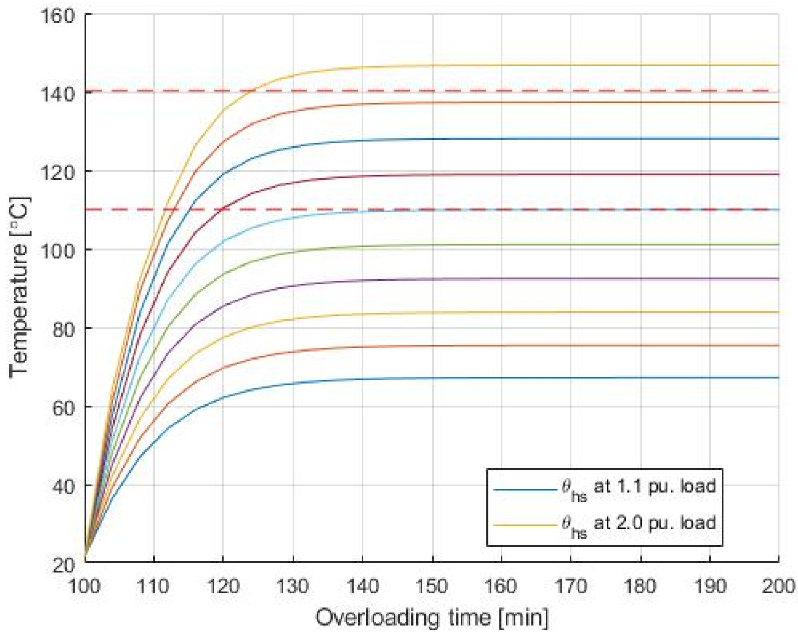

Figure 5.4: Hot-spot temperatures during overloading conditions. Overloads range from 1.1-2.0 pu. Lower red dashed line denotes 110°C and upper red dashed line denotes 140°C.

Looking at the lower red dashed line in Figure 5.4 above, the hot-spot temperature begins to exceed the reference temperature at 1.7 pu. load, which in turn results in thermal ageing occurring faster than nominal levels. Furthermore, the upper temperature threshold is exceeded at 2.0 pu. load, thus this load is not viable due to the risk of gas bubble formation in the transformer oil. 1.9 pu. is therefore the upper load limit that is safe to use continuously in these moderate cold weather conditions, with respect to temperature guidelines from industrial standards. However, this load step remains several steps higher than the recommended 1.5 pu. load from the industrial standards with respect to current loading.

5.2.4 Case 4: Chilling (0°C)

Increasing the ambient temperature to 0°C results in higher hot-spot temperatures, and the strain on the transformer will be increased further. Figure 5.5 below showcases the hot-spot temperature results under overloading conditions ranging from 1.1-1.9 pu. As before, the red dashed lines denote the reference operating temperature 110°C and the upper hot-spot temperature limit 140°C.

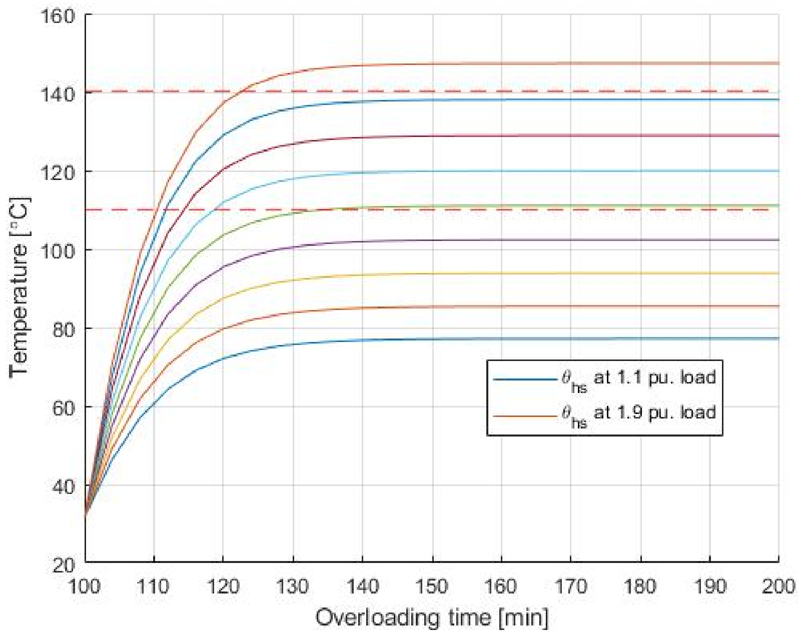

Figure 5.5: Hot-spot temperatures during overloading conditions. Overloads range from 1.1-1.9 pu. Lower red dashed line denotes 110°C and upper red dashed line denotes 140°C.

Looking at the lower red dashed line in Figure 5.5 above, the hot-spot temperature begins to exceed the reference temperature at 1.5 pu. load, which in turn results in thermal ageing occurring faster than nominal levels. Furthermore, the upper temperature threshold is exceeded at 1.9 pu. load, thus this load is not viable due to the risk of gas bubble formation in the transformer oil. 1.8 pu. is therefore the upper load limit that is safe to use continuously in these chilling weather conditions, with respect to temperature guidelines from industrial standards. However, this load step remains higher than the recommended 1.5 pu. load from the industrial standards with respect to current loading.

5.2.5 Case 5: Moderate warm (10°C)

Increasing the ambient temperature to 10°C results in higher hot-spot temperatures, and the strain on the transformer will be increased further. Figure 5.6 on below showcases the hot-spot temperature results under overloading conditions ranging from 1.1-1.8 pu. As before, the red dashed lines denote the reference operating temperature 110°C and the upper hot-spot temperature limit 140°C.

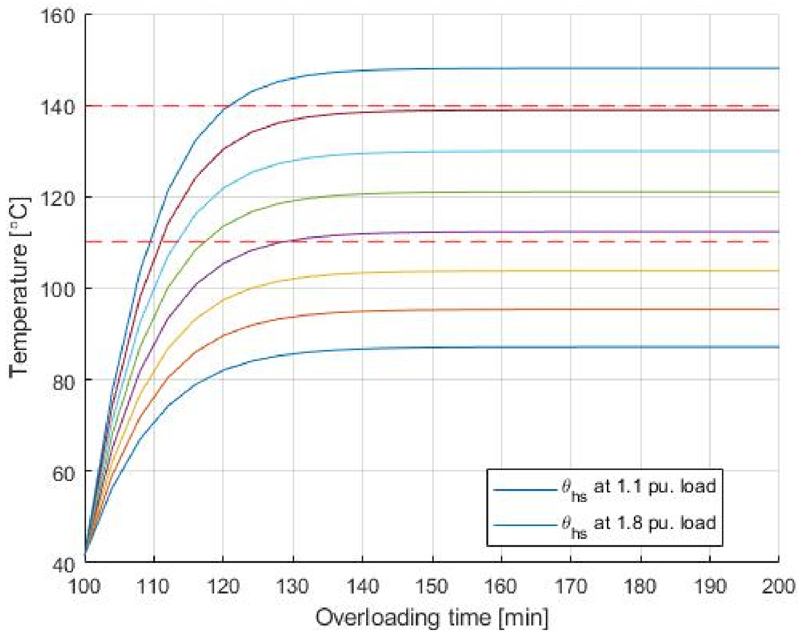

Figure 5.6: Hot-spot temperatures during overloading conditions. Overloads range from 1.1-1.8 pu. Lower red dashed line denotes 110°C and upper red dashed line denotes 140°C.

Looking at the lower red dashed line in Figure 5.6 above, the hot-spot temperature begins to exceed the reference temperature at 1.5 pu. load, which in turn results in thermal ageing occurring faster than nominal levels. Furthermore, the upper temperature threshold is exceeded at 1.9 pu. load, thus this load is not viable due to the risk of gas bubble formation in the transformer oil. 1.8 pu. is therefore the upper load limit that is safe to use continuously in these chilling weather conditions, with respect to temperature guidelines from industrial standards. However, this load step remains higher than the recommended 1.5 pu. load from the industrial standards with respect to current loading.

5.2.6 Case 6: Warm (20°C)

Increasing the ambient temperature to 20°C results in higher hot-spot temperatures, and the strain on the transformer will be increased further. Figure 5.7 below showcases the hot-spot temperature results under overloading conditions ranging from 1.1-1.7 pu. As before, the red dashed lines denote the reference operating temperature 110°C and the upper hot-spot temperature limit 140°C.

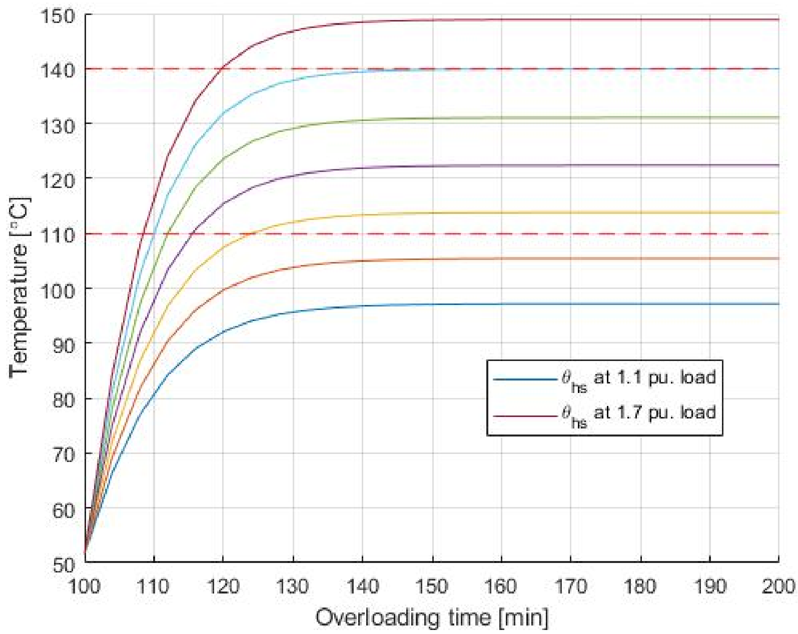

Figure 5.7: Hot-spot temperatures during overloading conditions. Overloads range from 1.1-1.7 pu. Lower red dashed line denotes 110°C and upper red dashed line denotes 140°C.

Looking at the lower red dashed line in Figure 5.7 above, the hot-spot temperature begins to exceed the reference temperature at 1.3 pu. load, which in turn results in thermal ageing occurring faster than nominal levels. Furthermore, the upper temperature threshold is exceeded at 1.7 pu. load, thus this load is not viable due to the risk of gas bubble formation in the transformer oil. 1.6 pu. load approaches steady-state by the upper temperature threshold. The load is strictly speaking viable according to the guidelines, but there could be a safety risk to continuously loading the transformer at the very brink of the threshold. Slight errors could result in the temperature exceeding the limit. This load step is also slightly higher than the recommended 1.5 pu. load from the industrial standards, with respect to current loading.

5.2.7 Case 7: Design condition (30°C)

Increasing the ambient temperature to 30°C results in higher hot-spot temperatures, and the strain on the transformer will be increased further. This ambient temperature is the reference for assigning the static rating of transformer designs. Figure 5.7 below showcases the hot-spot temperature results under overloading conditions ranging from 1.1-1.5 pu. As before, the red dashed lines denote the reference operating temperature 110°C and the upper hot-spot temperature limit 140°C.

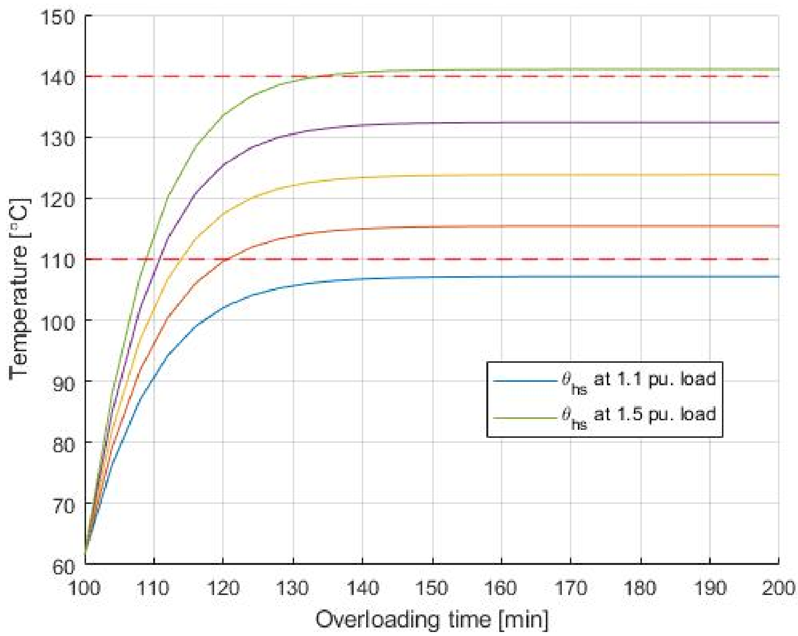

Figure 5.8: Hot-spot temperatures during overloading conditions. Overloads range from 1.1-1.5 pu. Lower red dashed line denotes 110°C and upper red dashed line denotes 140°C.

Looking at the lower red dashed line in Figure 5.8 above, the hot-spot temperature begins to exceed the reference temperature at 1.2 pu. load, which in turn results in thermal ageing occurring faster than nominal levels. Furthermore, the upper temperature threshold is exceeded at 1.5 pu. load, thus this load is not viable due to the risk of gas bubble formation in the transformer oil. 1.4 pu. is therefore the upper load limit that can be used continuously in these design conditions. Note that the load now adheres to the industrial standards with respect to current loading. It may be that the current loading recommendations provided by the industrial standards are chosen with the design conditions in mind, which would be a conservative guideline in colder regions like Norway.

5.2.8 Summary of steady-state numerical results

Table 5.3 below lists numerical results of the steady-state hot-spot temperatures for the different ambient temperatures at t = 200 minutes. The transformer can be safely run at operating temperatures below 140°C. Thus, the examined transformer can be overloaded continuously with up to 110% increased current, depending on the ambient temperature.

Table 5.3: Steady-state hot-spot temperature values at t = 200 minutes

θ_{amb} [°C]	**Load**	1.4	1.5	1.6	1.7	1.8	1.9	2.0	2.1	2.2
-30	θ_{hs}[°C]	72.4	81.1	89.9	98.9	108.1	117.3	126.7	136.3	145.9
-20	θ_{hs}[°C]	82.4	91.1	99.9	108.9	118.1	127.3	136.7	146.3	
-10	θ_{hs}[°C]	92.4	104.1	109.9	118.9	128.1	138.1	147.3		
0	θ_{hs}[°C]	102.4	111.1	119.9	128.9	138.1	147.3			
10	θ_{hs}[°C]	112.4	121.1	129.9	138.9	148.1				
20	θ_{hs}[°C]	131.1	139.9	148.9						
30	θ_{hs}[°C]	132.4	141.1							

5.3 Thermal ageing during 24 hours of overloading

In this section results from loss-of-life calculations performed by the simulations are presented and discussed. The examined transformer is the same 300 MVA transformer as in the previous section. The transformer is overloaded with 1.5 pu. for 24 hours in accordance with current loading guidelines from the industrial standards. As before, the overloading is initiated at t = 100 minutes. Loss-of-life calculations are performed with the four respective moisture and air conditions listed in Table 3.2 in Chapter 3.

5.3.1 Case 1: Extreme cold (-30°C)

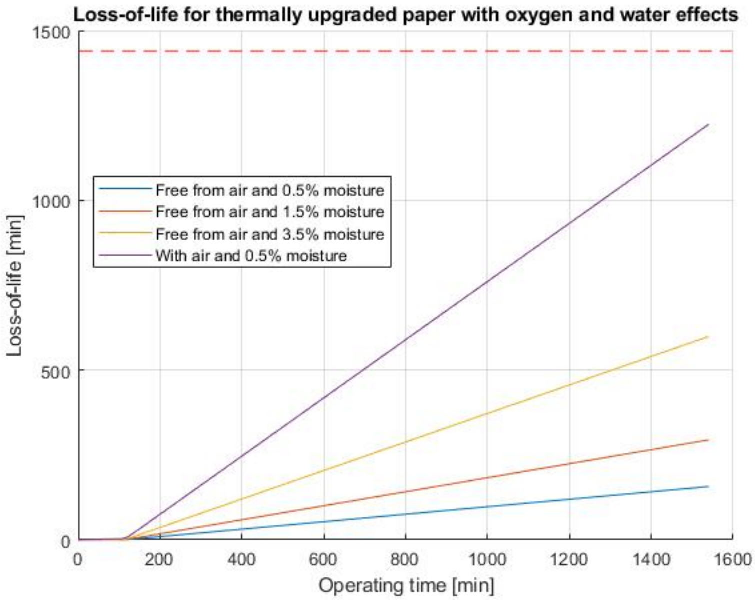

Figure 5.9: Loss-of-life with 1.5 pu. overloading for 24 hours. Red dashed line denotes loss-of-life equal to 1440 minutes or 24 hours.

In Figure 5.9 above, there is a dashed red line at the top of the graph. The dashed red line illustrates the loss-of-life equal to 1440 minutes or 24 hours. The line is there to indicate when the loss-of-life that occurs from operating the transformer at higher loads results in the transformer using more than its normal daily life. It is apparent that at this ambient temperature, the transformer does not reach this threshold when overloading at 1.5 pu. regardless of the condition of the paper insulation. Thus, the example transformer can be continuously loaded at 1.5 pu. in these extreme cold weather conditions. Table 5.4 below lists the loss-of-life after 24 hours of overloading.

Table 5.4: Loss-of-life after 1440 minutes or 24 hours overloading

Thermal conditions	Loss of life [min]
Free from air and 0.5% moisture	157
Free from air and 1.5% moisture	295
Free from air and 3.5% moisture	599
With air and 0.5% moisture	1224

5.3.2 Case 2: Cold (-20°C)

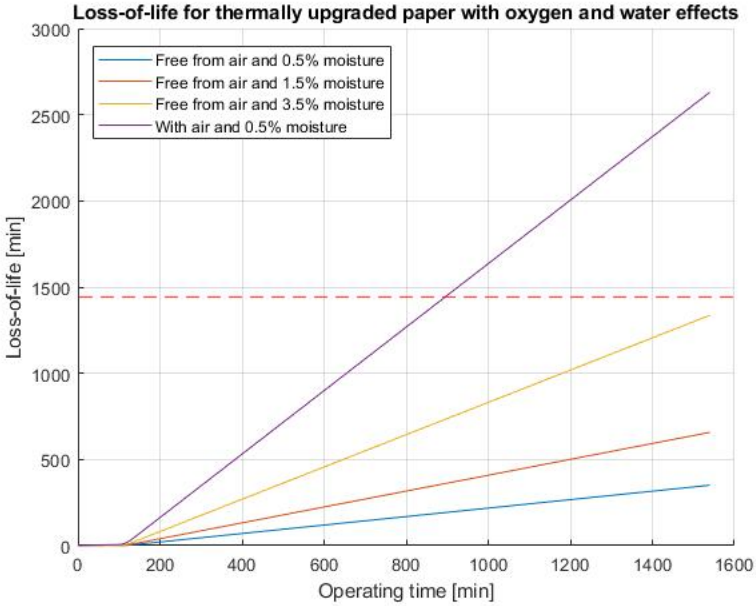

Figure 5.10: Loss-of-life with 1.5 pu. overloading for 24 hours. Red dashed line denotes loss-of-life equal to 1440 minutes or 24 hours.

By increasing the ambient temperature to -20°C, the increased hot-spot temperatures accelerate the ageing rate, as showcased in Figure 5.10. In this circumstance, the worst condition of the paper insulation exceeds the normal daily life. Table 5.5 below lists numerical results. In the worst case scenario, the paper insulation loses 2630 minutes of its lifespan after 1440 minutes or 24 hours of overloading. The transformer can still be overloaded continuously with no consequences at 1.5 pu. load, provided that the paper insulation is in good condition.

Table 5.5: Loss-of-life after 1440 minutes or 24 hours overloading

Thermal conditions	Loss of life [min]
Free from air and 0.5% moisture	351
Free from air and 1.5% moisture	657
Free from air and 3.5% moisture	1337
With air and 0.5% moisture	2630

5.3.3 Case 3: Moderate cold (-10°C)

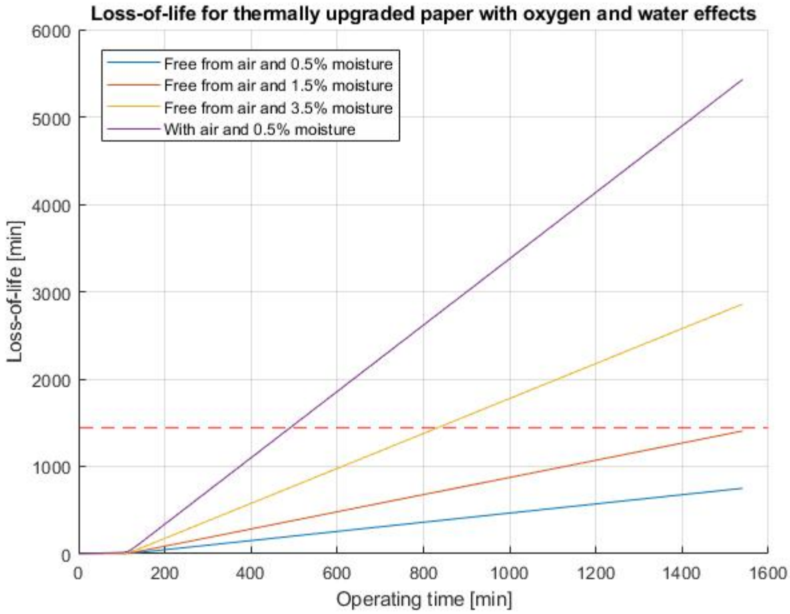

Figure 5.11: Loss-of-life with 1.5 pu. overloading for 24 hours. Red dashed line denotes loss-of-life equal to 1440 minutes or 24 hours.

Increasing the ambient temperature further to -10°C, results in the loss-of-life threshold being exceeded for the second-worst condition of the paper insulation material aswell. Table 5.6 below lists numerical results, showing that the paper loses 2858 minutes of its lifespan after 1440 minutes or 24 hours of overloading in the second-worst scenario. The transformer can still be continuously overloaded at 1.5 pu. with no consequences, provided the paper insulation is in good condition.

Table 5.6: Loss-of-life after 1440 minutes or 24 hours overloading

Thermal conditions	Loss of life [min]
Free from air and 0.5% moisture	750
Free from air and 1.5% moisture	1406
Free from air and 3.5% moisture	2858
With air and 0.5% moisture	5429

5.3.4 Case 4: Chilling (0°C)

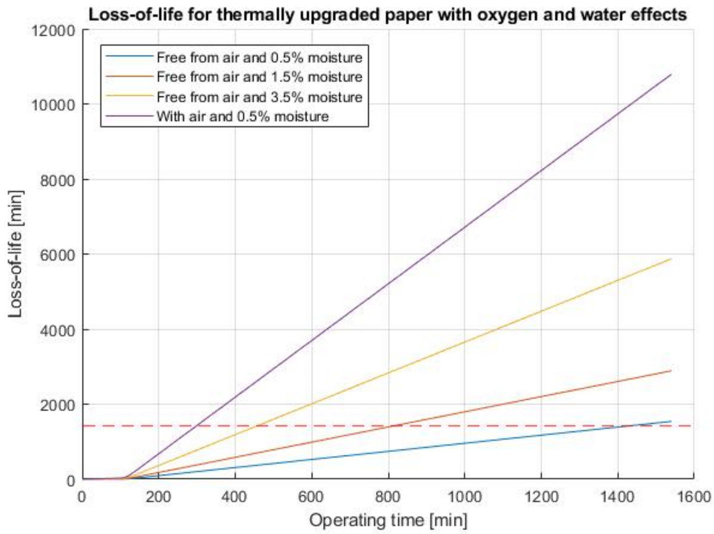

Figure 5.12: Loss-of-life with 1.5 pu. overloading for 24 hours. Red dashed line denotes loss-of-life equal to 1440 minutes or 24 hours.

Increasing the ambient temperature further to 0°C results in the loss-of-life threshold being exceeded regardless of the condition of the paper insulation at 1.5 pu. load, as seen in Figure 5.12. Table 5.7 below lists the numerical results, showing that under normal conditions, the paper insulation loses 1541 minutes of its lifespan after 1440 minutes or 24 hours of overloading. Thus, in order to utilize 1.5 pu. loading at 0°C ambient temperature and above, a time limit must be imposed if the life expectancy of the transformer is to be preserved.

Table 5.7: Loss-of-life after 1440 minutes or 24 hours overloading

Thermal conditions	Loss of life [min]
Free from air and 0.5% moisture	1541
Free from air and 1.5% moisture	2889
Free from air and 3.5% moisture	5874
With air and 0.5% moisture	10791

5.4 Additional remarks and validity of the methodology

In the presented simulation results, the 300 MVA transformer has been overloaded continuously at a constant load with a constant ambient temperature. In a real power system, the power demand and ambient weather conditions will change. That being said, the results that have been presented are useful in highlighting that the transformer can be overloaded significantly beyond its name-plate rating without jeopardizing its safety and thermal life expectancy.

It is not desirable to decrease the life expectancy of the transformer when discussing the use of dynamic ratings as they are conventionally defined, as the goal is to optimize the normal transformer loading. However, it does not mean that decreasing the life expectancy is completely out of bounds. The scope of the thermal ageing simulations examined a 24 hour time window. In the case of several days, weeks or months, the transformer could be overloaded for a series of days, accelerating the thermal ageing and increasing the loss-of-life. The transformer load can later be lowered in the time-frame to make up for the lost paper insulation life. Depending on the specific transformer, it may be advised to decrease the life expectancy of the transformer to some extent. Consider an older transformer that is scheduled to be replaced within a certain amount of years. Overloading the transformer would increase its usage in those remaining years, provided that a reduction in life expectancy does not speed up the need to replace the equipment faster than planned.

Based on the findings from the introduction study, one would assume that the simulation methodology in this thesis should in theory produce sufficiently accurate results. However, as with any simulation setup, the results can only be reliably accurate provided that the data parameters used are reliable. It is therefore of critical importance that reliable data is gathered as more studies and work is done on the topic of dynamic transformer ratings.

Chapter 6

Conclusion and future work

In this thesis, a simulation methodology to estimate transient temperatures and loss-of-life of paper insulation for dynamic transformer rating studies has been developed. Several case studies of loading a 300 MVA power transformer beyond its name-plate rating in various ambient temperatures have been presented.

Results show that the examined transformer can be overloaded continuously with up to 110% increased current, depending on the ambient temperature. The transformer can be operated safely under 140°C. Higher temperatures can lead to gas bubble formation in the transformer oil. Overloading with 50% and more increased current exceeds recommendations for current loading of large power transformers by present day industrial standards. As dynamic rating systems of transformers become more prevalent in the future, it is proposed that the current loading recommendations should be revised.

Thermal ageing studies suggest overloading with 50% increased current at 0°C ambient temperature and above reduces the life expectancy of the transformer. Therefore, a time limit must be introduced if the transformer capacity is to be preserved. Optimizing the paper insulation life is the main challenge in implementing dynamic transformer ratings. There is great potential for increasing capacity usage of transformers in cold weather regions like Norway.

Future work should focus on investigating intelligent ways to optimize the available paper insulation life of the transformer. Some suggestions include:

- Improve the proposed simulation methodology and conduct more studies with measurement data and/or physical lab experiments for validation.
- Develop a real-time dynamic rating system employing control system techniques such as model predictive control. If developed in Simulink, the simulation modules presented in this thesis could be re-used for this purpose.

Bibliography

[1] T. I. Kopperud, ”Dynamic rating of transformers,” Specialization project, Norwegian University of Science and Technology, Trondheim, 2020.

[2] T. Zarei, K. Morozovska, T. Laneryd, P. Hilber, M. Wihlén and O. Hansson, ”Reliability considerations and economic benefits of dynamic transformer rating for wind energy integration,” *Electrical Power and Energy Systems*, pp. 598-606, 2019.

[3] A. Safdarian, M. Z. Degefa, M. Fothu-Firuzabad, and M. Lehtonen, ”Benefits of real-time monitoring to distribution systems: Dynamic thermal rating,” *IEEE Transactions on Smart Grid*, vol. 6, no. 4, pp. 2023-2031, 2015.

[4] D. A. Douglass, D. C. Lawry, A. A. Edris, and E. C. Bascom, ”Dynamic thermal ratings realize circuit load limits,” *IEEE Computer Applications in Power*, vol. 13, no. 1, pp. 38-44, 2000.

[5] A. Michiorri, P. Taylor, S. Jupe and C. Berry, ”Investigation into the influence of environmental conditions on power system ratings”, *Proceedings of the Institution of Mechnical Engineers, Part A: Journal of Power and Energy*, pp.743-757, 2009.

[6] D. Susa and M. Lehtonen, ”Dynamic thermal modeling of power transformers: Further development - Part I,” *IEEE Transactions on Power Delivery*, vol. 21, no. 4, pp. 1961-2006, 2006.

[7] Institute of Electrical and IEEE Electronics Engineers. *C57.91-2011 - IEEE guide for loading mineral-oil-immersed transformers and step voltage regulators*, 2011.

[8] Elettromeccanica Colombo, Oil immersed power transformers, 2021, Available: `http://www.elettrocolombo.com/en/products/trasformatori_di_potenza/trasformatori_di_potenza_in_olio`

[9] S. V. Kulkarni and S. A. Khaparde, *Transformer Engineering: Design and Practice*, 1st edition, CRC Press, 2004.

[10] M. J. Heathcote, *J & P Transformer Book,* 13th edition, Newnes, 2007.

[11] J. Perez, ”Fundamental principles of transformer thermal loading and protection,” *11th IET International Conference on Developments in Power Systems*, 2012.

[12] J. Perez, ”Fundamental principles of transformer thermal loading and protection,” *63rd Annual Conference for Protective Relay Engineers,* 2010.

[13] D. A. Douglass and A.-A. Edris, ”Real-time monitoring and dynamic thermal rating of power transmission circuits,” *IEEE Transactions on Power Delivery*, vol. 11, no. 3, pp. 1407-1418, 1996.

[14] Slaters electricals, Parsons Peebles DTL 800kVA 11000/3300V Transformer, 2021, Available: `https://slaters-electricals.com/stock/transformers/distribution-transformers/parsons-peebles-dtl-800kva-11000-3300v-transformer/`

[15] M. F. Lachman, P. J. Griffin, W. Walter and A Wilson. ”Real-time dynamic loading and thermal diagnostic of power transformers,” *IEEE Transactions on Power Delivery*, vol. 18, no. 1, pp. 142-148, 2003.

[16] T. S. Jalal, N. Rashid, B. van Vliet, ”Implementation of dynamic transformer rating in a distribution network”, *IEEE International Conference on Power System Technology*, 2012.

[17] ”IEC 60076-7:2018 Power Transformers Part 7: Loading guide for mineral-oil-immersed power transformers,” *International Electrotechnical Commission*, 2018.

[18] K. Morozovska, ”Dynamic rating with applications to renewable energy,” Ph.D. dissertation, KTH Royal Institute of Technology, 2020.

[19] I. Daminov, A. Prokhorov, R. Caire, M-C. Alvarez-Herault, ”Receding horizon algorithm for dynamic transformer rating and its application for real-time economic dispatch,” *IEEE Milan PowerTech*, 2019.

[20] ”IEC 60076-7:2018 Power Transformers Part 7: Loading guide for mineral-oil-immersed power transformers,” *International Electrotechnical Commission*, 2018.

[21] D. Villacci, G. Bontempi, A. Vaccaro and M. Birattari, ”The role of learning methods in the dynamic assessment of power components loading capability,” *IEEE Transactions on Industrial Electronics*, vol. 52, no. 1, pp. 280-290, 2005.

[22] L. Li, W. Liu, H. Chen and X. Liu, ”Prediction of oil flow and temperature distribution of transformer winding based on multi-field coupled approach”, *The 14th IET International Conference on AC and DC Power Transmission*, vol. 51, no. 3, pp.2007-2012, 2018

[23] M. Djamali and S. Tenbohlen, ”Hundred years of experience in the dynamic thermal modelling of power transformers”, *IET Generation, Transmission Distribution*, vol. 11, no. 11, pp.-2731-2739, 2017.

[24] S. Jupe, M. Barlett and K. Jackson, ”Dynamic thermal ratings: The state of the art”, *21st International Conference on Electricity Distribution*, 2011.

[25] W. Chen, J. Liu, Y. Wang, L. Liang, J. Zhao and Y. Yue, ”The measuring method for internal temperature of power transformers based on FBG sensors”, *International Conference on High Voltage Engineering and Application*, 2008.

[26] S. Agboza, ”Dynamisk termisk modellering av krafttransformatorer,” M.S. Thesis, Norwegian University of Science and Technology, Trondheim, 2020.

[27] G. Swift, T. S. Molinski and W. Lehn, ”A fundamental approach to transformer thermal modeling - Part I: Theory and equivalent circuit,” *IEEE Transactions on Power Delivery*, vol. 16, no. 2, 2001.

[28] G. Swift, ”A fundamental approach to transformer thermal modeling - Part II: Field verification,” *IEEE Transactions on Power Delivery*, vol. 16, no. 2, 2001.

[29] L. W. Pierce, ”Predicting liquid filled transformer loading capability,” *IEEE Transactions on Industry Applications*, vol. 30, no. 1, pp. 170-178, 1994.

[30] D. Susa, ”Dynamic thermal modelling of power transformers,” Ph.D dissertation, Helsinki University of Technology, 2005.

[31] ”Cigré Brochure 323 - Ageing of cellulose in mineral-oil insulated transformers,” TF D1.01.10, 2007.

[32] L. E. Lundgaard, K. B. Lilland, D. Linhjell, D. Susa, M-H.G. Ese, C. M. Selsbak, M. Kes and C. Lesaint, ”Transformer Windings - Ageing, diagnosis and asset management,” Sintef Energy Research, Trondheim, Norway, TR A7099, 18.09.2015.

[33] D. Susa. Personal phone correspondence, 2020.

Appendix A

Mathematical derivation of Agboza model

In this Appendix, a full review of the step by step mathematical procedure to derive the final equations used in Agboza's NTNU model [26] is presented. This same appendix can be found in the autumn specialization work with minor differences in [1].

A.1 Bottom-oil temperature

Table A.1: List of symbols used in bottom-oil modeling

Symbol	Description	SI-unit
q_{fe}	No-load losses	[W]
q_{cu}	Load losses	[W]
$q_{cu,R}$	Rated load losses	[W]
C_{th-oil}	Thermal capacitance of oil	[J/°C]
θ_{boil}	Bottom-oil temperature	[°C]
θ_{amb}	Ambient temperature	[°C]
$R_{th-boil-air,R}$	Non-linear thermal resistance between bottom-oil and air at rated load	[°C/W]
n	Constant that defines non-linear heat transfer from oil to air	
$\Delta\theta_{boil,R}$	Rated bottom-oil temperature rise above ambient temperature	
τ_{boil}	Bottom-oil time constant	
R	Relation between rated load losses and no-load losses	
I	Load current	[A]
I_R	Rated current	[A]
K	Load factor	
t	Time step	

The thermal circuit for the bottom-oil temperature may be expressed by Equation A.1. A complete list of symbols used in the procedure is given in Table A.1.

$$q_{fe} + q_{cu} = C_{th-oil} \cdot \frac{d\theta_{boil}}{dt} + \frac{(\theta_{boil} - \theta_{amb})^{\frac{1}{n}}}{R_{th-boil-air,R}} \tag{A.1}$$

The equation is to be derived further before one may use it. First, some additional terms are defined; the rated bottom-oil temperature rise above the ambient temperature $\Delta\theta_{boil,R}$, the bottom-oil time constant τ_{boil}, and the ratio between rated load-losses and no-load losses R:

$$(\Delta\theta_{boil,R})^{\frac{1}{n}} = (q_{fe} + q_{cuR}) \cdot R_{th-boil-air,R} \tag{A.2}$$

$$\tau_{boil} = R_{th-boil-air,R} \cdot C_{th-oil} \tag{A.3}$$

$$R = \frac{q_{cu,R}}{q_{fe}} \tag{A.4}$$

Next, a load factor K is introduced in Equation A.5, and the relation between the load-losses and current is introduced in Equation A.6.

$$K_{pu} = \frac{I}{I_R} \tag{A.5}$$

$$\frac{q_{cu}}{q_{cu,R}} = (\frac{I}{I_R})^2 \tag{A.6}$$

By combining the two relations, one may then express the load-losses q_{cu} as a function of the rated load losses and the load factor.

$$q_{cu} = q_{cu,R} \cdot K_{pu}^2 \tag{A.7}$$

Now that the necessary new terms have been introduced, further deriving can be done to the original Equation A.1. First, the expression is multiplied with $R_{th-boil-air,R}$ and subsequently the time constant τ_{boil} is inserted, resulting in:

$$(q_{fe} + q_{cu}) \cdot R_{th-boil-air,R} = \tau_{boil} \cdot \frac{d\theta_{boil}}{dt} + (\theta_{boil} - \theta_{amb})^{\frac{1}{n}} \tag{A.8}$$

Next, Equation A.2 is rewritten as an expression for $R_{th-boil-air,R}$, and $R_{th-boil-air,R}$ is then replaced in Equation A.8, resulting in:

$$\frac{q_{fe} + q_{cu}}{(q_{fe} + q_{cu})_R} \cdot (\Delta\theta_{boil,R})^{\frac{1}{n}} = \tau_{boil} \cdot \frac{d\theta_{boil}}{dt} + (\theta_{boil} - \theta_a mb)^{\frac{1}{n}} \tag{A.9}$$

Next, Equation A.7 is inserted, and the expression is multipled with $\frac{1}{q_{fe}}$, resulting in:

$$\frac{1 + \frac{q_{cu,R}}{q_{fe}} \cdot K_{pu}^2}{1 + \frac{q_{cu,R}}{q_{fe}}} \cdot (\Delta\theta_{boil,R})^{\frac{1}{n}} = \tau_{boil} \cdot \frac{d\theta_{boil}}{dt} + (\theta_{boil} - \theta_{amb})^{\frac{1}{n}} \tag{A.10}$$

Finally, the relation between the load and no-load losses R is inserted, resulting in the final expression that is more practical to use when calculating the bottom-oil temperature.

$$\frac{1 + K_{pu}^2 \cdot R}{1 + R} \cdot (\Delta\theta_{boil,R})^{\frac{1}{n}} = \tau_{boil} \cdot \frac{d\theta_{boil}}{dt} + (\theta_{boil} - \theta_{amb})^{\frac{1}{n}} \tag{A.11}$$

A.2 Hot-spot temperature

Table A.2: List of symbols used in hot-spot temperature modeling

Symbol	Description	SI-unit
$\Delta\theta_{hs-boil}$	Hot-spot rise above bottom-oil temperature gradient	
$C^{'''}$	Constant	
p	Constant	
q_{wdn}	Winding losses	[W]
$R_{th-hs-boil}$	Thermal resistance	[°C/W]
q_{cu}	Load losses	
$q_{cu,R}$	Rated load losses	
m	Constant that defines non-linear heat transfer from winding to oil	
θ_{hs}	Hot-spot temperature	[°C]
θ_{boil}	Bottom-oil temperature	[°C]
C_{th-wdn}	Winding thermal capacitance	[J/°C]
I	Load current	[A]
I_R	Rated current	[A]
t	Time step	

The thermal circuit describing the hot-spot temperature may be expressed as the following differential equation:

$$q_{cu} = C_{th-wdn} \cdot \frac{d\theta_{hs}}{dt} + \frac{(\theta_{hs} - +\theta_{boil})^{\frac{1}{m}}}{R_{th-hs-boil,R}} \tag{A.12}$$

As with the bottom-oil modeling, first some new terms are introduced; the rated hot-spot temperature rise over bottom-oil temperature $\Delta\theta_{hs-boil,R}$, the winding time constant τ_{wdn}, and the load factor K.

$$(\Delta\theta_{hs-boil,R})^{\frac{1}{m}} = q_{cu,R} \cdot R_{th-hs-boil,R} \tag{A.13}$$

$$\tau_{wdn} = R_{th-hs-boil,R} \cdot C_{th-wdn} \tag{A.14}$$

$$K_{pu} = \frac{I}{I_R} \tag{A.15}$$

As before, the relation between the load losses and the currents is introduced and combined with the load factor K to obtain an expression for the load losses as a function of the rated load losses and the load factor.

$$\frac{q_{cu}}{q_{cu,R}} = (\frac{I}{I_R})^2 \tag{A.16}$$

$$q_{cu} = q_{cu,R} \cdot K_{pu}^2 \tag{A.17}$$

Furthermore, by converting the load losses on the left side of Equation A.17 to per unit form, the rated load losses are canceled out. This results in the following relation between the per unit load losses and load factor:

$$q_{cu,pu} = K_{pu}^2 \tag{A.18}$$

Additionally, an expression for the natural heat transfer between the top of the surface of the winding insulation and the bottom-oil temperature is introduced:

$$\Delta\theta_{hs-boil} = C^{'''} \cdot q_{cu}^p \tag{A.19}$$

where:

- $C^{'''}$ and p are constants. p is provided by the IEEE loading guide [7]
- q_{wdn} are winding load-losses [W]

Next, the heat transfer relation for the hot-spot rise to bottom-oil temperature gradient is introduced:

$$(\Delta\theta_{hs-boil})^{\frac{1}{m}} = R_{th-hs-boil} \cdot q_{cu} \tag{A.20}$$

By combining Equation A.19 and Equation A.20, an expression for the thermal resistance between the top surface of the winding insulation and the bottom-oil temperature may be described by the following:

$$R_{th-hs-boil} = \frac{(\Delta\theta_{hs-boil})^{\frac{1}{m}}}{q_{cu}} = \frac{(C^{'''} \cdot q_{cu}^p)^{\frac{1}{m}}}{q_{cu}} = C^{'''} \cdot q_{cu}^{\frac{1}{m}-1} \tag{A.21}$$

The thermal resistance is then converted into per unit form:

$$R_{th-hs-boil,pu} = \frac{q_{cu}^{\frac{p}{m}-1}}{q_{cu,R}^{\frac{p}{m}-1}} = q_{cu,pu}^{\frac{p}{m}-1} \tag{A.22}$$

Now that the necessary terms and relations have been introduced, the original Equation A.12 can be derived further, starting by multiplying with $R_{th-hs-boil}$.

$$q_{cu} \cdot R_{th-hs-boil} = C_{th-wdn} \cdot R_{th-hs-boil} \cdot \frac{d\theta_{hs}}{dt} + (\theta_{hs} - \theta_{boil})^{\frac{1}{m}} \tag{A.23}$$

Next, q_{cu} and $R_{th-hs-boil}$ are converted to per unit form, resulting in the following:

$$q_{cu,pu} \cdot q_{cu,R} \cdot R_{th-hs-boil,pu} \cdot R_{th-hs-boil,R} = C_{th-wdn} \cdot R_{th-hs-boil} \cdot \frac{d\theta_{hs}}{dt} + (\theta_{hs} - \theta_{boil})^{\frac{1}{m}} \tag{A.24}$$

Next, Equations A.13, A.14 and A.22 are inserted, resulting in:

$$q_{cu,pu}^{\frac{p}{m}} \cdot (\Delta\theta_{hs-boil,R})^{\frac{1}{m}} = \tau_{wdn} \cdot \frac{d\theta_{hs}}{dt} + (\theta_{hs} - \theta_{boil})^{\frac{1}{m}} \tag{A.25}$$

Finally, the load factor K is inserted from Equation A.18, resulting in the final expression that is more practical to use when calculating the hot-spot temperature.

$$K_{pu}^{\frac{2p}{m}} \cdot (\Delta\theta_{hs-boil,R})^{\frac{1}{m}} = \tau_{wdn} \cdot \frac{d\theta_{hs}}{dt} + (\theta_{hs} - \theta_{boil})^{\frac{1}{m}} \tag{A.26}$$

Appendix B

250 MVA power transformer data

- Ambient temperature θ_{amb} = 25.6°C
- Ratio between load-losses and no-load losses at rated voltage R = 1000
- Bottom-oil time constant τ_{boil} = 150 [min]
- Winding time constant τ_{wdn} = 18 [min]
- Oil exponent n = 0.9
- Winding exponents m = 0.8 and p = 0.5
- Hot-spot rise above ambient temperature gradient at rated voltage $\Delta\theta_{boil,R}$ = 16 [K]
- Hot-spot rise above bottom-oil temperature gradient at rated voltage $\Delta\theta_{hs-boil,R}$ = 46.2 [K]

Appendix C

300 MVA power transformer data

- Mass of oil m_{oil} = 62700 [kg]
- Mass of tank and fittings m_t = 59700 [kg]
- Mass of tank and fittings m_{fe} = 141000 [kg]
- Mass of coil assembly m_{wdn} = 70800 [kg]
- Heat capacity of winding material c_{wdn} = 390 [J/kg/°C]
- Heat capacity of core c_{fe} = 468 [J/kg/°C]
- Heat capacity of tank and fittings c_t = 468 [J/kg/°C]
- Heat capacity of oil c_{oil} = 1800 [J/kg/°C]
- Correction factor for oil in cooling modes k_{oil} = 1
- Thermal capacity of oil C_{th-oil} = $2.34 \cdot 10^8$
- Average oil rise temperature gradient $\Delta\theta_{avg,R}$ = 33.35 [K]
- Total losses q_tot, R = 669500 [W] R = 1000
- Bottom-oil time constant τ_{boil} = 195 [min]
- Winding time constant τ_{wdn} = 22.3 [min] for high-voltage winding
- Oil exponent n = 0.8
- Winding exponents m = 0.8 and p = 0.5
- Bottom-oil rise temperature gradient at rated voltage $\Delta\theta_{boil,R}$ = 18 [K]
- Hot-spot rise above bottom-oil temperature gradient at rated voltage $\Delta\theta_{hs-boil,R}$ = 51.1 [K] for high-voltage winding

Appendix D

Matlab Source Code

```matlab
clear
clc
close all

%% DTR simulation script
% Version 1.2 % Date: 09.06.21
% Author: Trond Ivar Kopperud

%% Define load/temperature if constant load/temperature is used
theta_amb = 10;  %% Ambient temperature [degree celsius] if constant ambient temperature is used
load_factor = 1.0; %% Load factor [p.u.] if constant load is used. Note: In this thesis work constant load is not used.

%% Define fixed variables used in thermal models
R = 1000; %% Relation between load losses and no-load losses during nominal operation
tau_boil = 19.5; %% Time constant of bottom-oil [min]
tau_wdn = 22.3; %% Time constant of winding [min]
n = 0.8; %% Oil constant
m = 0.8; p = 0.5; %% Winding constants
delta_boil_R = 18; %% Nominal bottom-oil temperature increase over ambient temperature [K]
delta_hs_boil_R = 51.1; %% Nominal hot-spot temperature rise over bottom-oil temperature [K]

%% Initial conditions for integrating temperature derivatives
initial_theta_boil = 30; %% Initial value of bottom-oil temperature [degree celsius]
initial_theta_hst = 40;  %% Initial value of hot-spot temperature [degree celsius]
```

```
%% Define parameters related to air and moisture effects on
    paper insulation
%% Thermally Upgraded paper
%% Case I
% Free from air and 0.5% moisture
E_a_t = 86000;       % Activation energy for thermally-
    upgraded paper
E_a_r_t = 86000;     % Rated activation energy for
    thermally-upgraded paper
A_t = 1.6*10^4;      % Environmental factor for thermally-
    upgraded
A_r_t = 1.6*10^4;    % Rated Environmental factor for
    thermally-upgraded paper
% Rated values are set as 'Free from air and 0.5% moisture'
    category from IEC.

%% Case II
% Free from air and 1.5% moisture
E_a_t2 = 86000;      % Activation energy for thermally-
    upgraded paper
A_t2 = 3.0*10^4;     % Environmental factor for thermally-
    upgraded

%% Case III
% Free from air and 3.5% moisture
E_a_t3 = 86000;      % Activation energy for thermally-
    upgraded paper
A_t3 = 6.1*10^4;     % Environmental factor for thermally-
    upgraded

%% Case IV
% With air and 0.5% moisture
E_a_t4 = 82000;      % Activation energy for thermally-
    upgraded paper
A_t4 = 3.2*10^4;     % Environmental factor for thermally-
    upgraded

%% Run simulation
tFinal = 1540; % Simulation runtime
ThermalSim = sim('Simulink_DRT.slx'); % Run simulink model

%% Extracting data generated by simulink model.
%% Extracting data from signal x
```

```
% Signal x contains bottom-oil and hot-spot temperature data
ThermalSignal = ThermalSim.yout.getElement('x'); % Extract signal 'x' from simulink model
t = ThermalSignal.Values.Time;                   % Extract time values
theta_boil  = ThermalSignal.Values.Data(:,1);    % Extract Bottom-oil temperature data
theta_hst   = ThermalSignal.Values.Data(:,2);    % Extract Hot-spot temperature data

%% Extracting data from signal y
% Signal y contains loss-of-life data
ThermalSignal2 = ThermalSim.yout.getElement('y');  % Extract signal 'y' from Simulink
t2 = ThermalSignal2.Values.Time;                    % Extract time values
LOL_case2_t = ThermalSignal2.Values.Data(:,1);      % Extract loss of life data for case I
LOL_case3_t = ThermalSignal2.Values.Data(:,2);      % Extract loss of life data for case II
LOL_case4_t = ThermalSignal2.Values.Data(:,3);      % Extract loss of life data for case III
LOL_case5_t = ThermalSignal2.Values.Data(:,4);      % Extract loss of life data for case IV

%% Post-processing data

% Plot Hot-spot and bottom-oil temperatures
figure
 hold on
 plot(t, theta_hst)
 plot(t, theta_boil)
 xlabel('Time [min]')
 ylabel('\theta_{boil} [\circC]')
 grid on
 title('Hot-spot and bottom-oil temperatures')
 legend('\theta_{hs}', '\theta_{boil}', 'Location', 'best')

% Plot loss-of-life data
 figure
  hold on
  plot(t2, LOL_case2_t)
  plot(t2, LOL_case3_t)
  plot(t2, LOL_case4_t)
```

```matlab
plot(t2, LOL_case5_t)
h = yline(1440, 'r--', 'LineWidth', 1);
xlabel('Operating time [min]')
ylabel('Loss-of-life [min]')
grid on
title('Loss-of-life for thermally upgraded paper with oxygen and water effects')
legend('Free from air and 0.5% moisture', 'Free from air and 1.5% moisture', 'Free from air and 3.5% moisture', 'With air and 0.5% moisture', 'Location', 'best')


% Export Hot-spot temperature data to Excel sheet for further analysis.
col_header ={'t','hspot'};
xlswrite('data.xlsx', col_header,'Sheet1','A1');
xlswrite('data.xlsx',[t(:),theta_hst(:)],'Sheet1','A2');

%% Print numerical values in Matlab command window
[t-100 LOL_case2_t LOL_case3_t LOL_case4_t LOL_case5_t] % Print loss-of-life values

%% Comment:
% Note that 100 is subtracted from printed time values because the
% first 100 time steps are used as a ramp-up time in the simulation prior
% to initating overloading.
```